

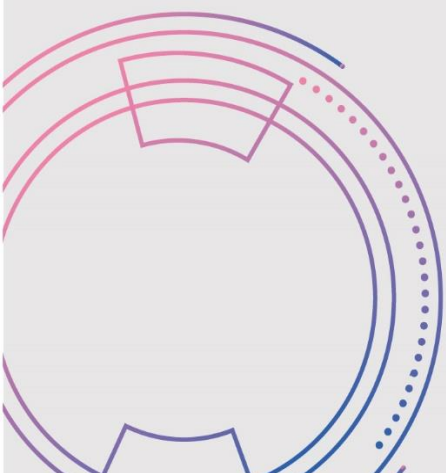


**Firat University
Journal of Experimental
and Computational
Engineering**

Volume: 2

Issues: 1

Year: 2023



Owner

On Behalf of Firat University

Rector

Prof. Dr. Fahrettin GÖKTAŞ

Editor-in-Chief

Prof. Dr. Mehmet YILMAZ, Firat University, Turkey

Vice Editor-in-Chief

Prof. Dr. Ebru AKPINAR, Firat University, Turkey

Prof. Dr. Ragıp İNCE, Firat University, Turkey

Prof. Dr. Levent TAŞÇI, Firat University, Turkey

Prof. Dr. Yakup DEMİR, Firat University, Turkey

Prof. Dr. Mete Onur KAMAN, Firat University, Turkey

Assoc. Prof. Dr. Erkut YALÇIN, Firat University, Turkey

Editorial Advisory Board

Prof. Dr. Abdulkadir Cüneyt AYDIN, Atatürk University, Turkey

Prof. Dr. Abdussamet ARSLAN, Gazi University, Turkey

Prof. Dr. Ahmet ŞAŞMAZ, Firat University, Turkey

Prof. Dr. Arif GÜLTEN, Firat University, Turkey

Prof. Dr. Baha Vural KÖK, Firat University, Turkey

Prof. Dr. Bilal ALATAŞ, Firat University, Turkey

Prof. Dr. Erhan AKIN, Firat University, Turkey

Prof. Dr. Erkan KÖSE, Nuh Naci Yazgan University, Turkey

Prof. Dr. Filiz KAR, Firat University, Turkey

Prof. Dr. Hasan SOFUOĞLU, Karadeniz Technical University, Turkey

Prof. Dr. İhsan DAĞTEKİN, Firat University, Turkey

Prof. Dr. İsmail Hakkı ALTAŞ, Karadeniz Technical University, Turkey

Prof. Dr. Kazım TÜRK, İnönü University, Turkey

Prof. Dr. M. Şaban TANYILDIZI, Firat University, Turkey

Prof. Dr. Mehmet KARAKÖSE, Firat University, Turkey

Prof. Dr. Mehtap MURATOĞLU, Firat University, Turkey

Prof. Dr. Nevin ÇELİK, Firat University, Turkey

Prof. Dr. Oğuz GÜNGÖR, Ankara University, Turkey

Prof. Dr. Oğuz YAKUT, Firat University, Turkey

Prof. Dr. Özge Kaya HANAY, Firat University, Turkey

Prof. Dr. Paki TURGUT, İnönü University, Turkey

Prof. Dr. Selçuk ÇEBİ, Yıldız Technical University, Turkey

Prof. Dr. Taner ALATAŞ, Firat University, Turkey

Prof. Dr. Yusuf AYVAZ, Yıldız Technical University, Turkey

Assoc. Prof. Dr. Fatih ÖZYURT, Firat University, Turkey

Editorial Board

Prof. Dr. Mehmet YILMAZ (Editor-in-Chief)	Civil Engineering
Prof. Dr. Ebru AKPINAR (Vice Editor-in-Chief)	Mechanical Engineering
Prof. Dr. Ragıp İNCE (Vice Editor-in-Chief)	Civil Engineering
Prof. Dr. Levent TAŞÇI (Vice Editor-in-Chief)	Civil Engineering
Prof. Dr. Yakup DEMİR (Vice Editor-in-Chief)	Electrical-Electronics Engineering
Prof. Dr. Mete Onur KAMAN (Vice Editor-in-Chief)	Mechanical Engineering
Assoc. Prof. Dr. Erkut YALÇIN (Vice Editor-in-Chief)	Civil Engineering
Prof. Dr. Abdullah Hilmi LAV	Civil Engineering
Prof. Dr. Ali TOPAL	Civil Engineering
Prof. Dr. Ali YAZICI	Software Engineering
Prof. Dr. Arif GAYDAROV	Chemical Engineering
Prof. Dr. Ayşe Vildan BEŞE	Chemical Engineering
Prof. Dr. Bilge Hilal CADIRCI EFELİ	Bioengineering
Prof. Dr. Ertan EVİN	Mechanical Engineering
Prof. Dr. Evren Meltem TOYGAR	Mechanical Engineering
Prof. Dr. Gülşad Uslu ŞENEL	Environmental Engineering
Prof. Dr. Kadir TURAN	Mechanical Engineering
Prof. Dr. H. Soner ALTUNDOĞAN	Bioengineering
Prof. Dr. Mehmet Deniz TURAN	Metallurgy and Materials Engineering
Prof. Dr. Mehmet YETMEZ	Mechanical Engineering
Prof. Dr. Murat ELİBOL	Bioengineering
Prof. Dr. Mustafa YANALAK	Geodesy and Photog. Engineering
Prof. Dr. Nicola TARQUE	Civil Engineering
Prof. Dr. Nuno MENDES	Mechanical Engineering
Prof. Dr. Rashid NADİROV	Chemical
Prof. Dr. Serdar Ethem HAMAMCI	Electrical-Electronics Engineering
Prof. Dr. Vizureanu PETRICA	Material Processing Technologies
Prof. Dr. VLadimir RYBAKOV	Mathematics and Computer Science
Assoc. Prof. Dr. Alvaro Garcia HERNANDEZ	Civil Engineering
Assoc. Prof. Dr. Baigenzhenov OMİRSERİK	Metallurgical Engineering
Assoc. Prof. Dr. Ebru DURAL	Civil Engineering
Assoc. Prof. Dr. Edip AVŞAR	Environmental Engineering
Assoc. Prof. Dr. Ersin Yener YAZICI	Mining Engineering
Assoc. Prof. Dr. Fatih ÇETİŞLİ	Civil Engineering
Assoc. Prof. Dr. Jülide ÖNER	Civil Engineering
Assoc. Prof. Dr. Marcin SAJDAK	Environmental Engineering and Energy
Assoc. Prof. Dr. Ömer GÖKKUŞ	Environmental Engineering
Assoc. Prof. Dr. Serdar ÇARBAŞ	Civil Engineering
Assoc. Prof. Dr. Tacettin GEÇKİL	Civil Engineering
Assoc. Prof. Dr. Erkut YALÇIN	Civil Engineering
Assist. Prof. Dr. Alvaro Aracena CAIPA	Chemical Engineering
Assist. Prof. Dr. Bahadır YILMAZ	Civil Engineering
Assist. Prof. Dr. Durmuş YARIMPABUÇ	Mathematics
Assist. Prof. Dr. Serap KOÇ	Mechanical Engineering
Assist. Prof. Dr. Ömer Saltuk BÖLÜKBAŞI	Metallurgy and Materials Engineering
Assist. Prof. Dr. Özlem AYDIN	Fod Engineering
Dr. Amilton Barbosa Botelho JUNİOR	Chemical Engineering
Dr. Norman TORO	Metallurgical Engineering
Res. Assist. Dr. Dragana BOZIC	Mining and Metallurgy Institute
Res. Assist. Dr. Jelena MİLOJKOVIĆ	Mineral Raw Materials Tech. Institute
Res. Assist. Dr. Serkan ERDEM	Civil Engineering
Res. Assist. Dr. Ulaş Baran BALOĞLU	Computer Engineering
Res. Assist. Shoeleh ASSEMI	Material Engineering
Lecturer Abdullah Gökhan TUĞAN (Language Editor)	English Language Teaching
Mustafa Gani GENÇER (Language Editor)	English Language Teaching
Res. Assist. Dr. Özge Erdoğan YAMAÇ (Pub. Coordinators)	Civil Engineering
Res. Assist. Beyza Furtana YALÇIN (Secretariat)	Civil Engineering

Composition

Hakan YURDAKUL

Correspondence Address

Firat University Faculty of Engineering Journal of Experimental and Computational Engineering Publishing Coordinatorship
23119 Elazığ/TÜRKİYE

E-mail: fujece@firat.edu.tr

Web page: <http://fujece.firat.edu.tr/>

Firat University Journal of Experimental and Computational Engineering a peer-reviewed journal.

CONTENTS

Behaviour of a strip footing adjacent to the existing supported excavation (Research Article) Mevcut destekli kazıya bitişik bir şerit temelin davranışı (Araştırma Makalesi)	
Mesut GÖR, Nichirvan Ramadhan TAHER, Hüseyin Suha AKSOY	1
Determination of thermophysical properties of Ficus elastica leaves reinforced epoxy composite (Research Article) Kauçuk ağacı (Ficus elastica) yaprağı takviyeli epoksi kompozitin termofiziksel özelliklerinin belirlenmesi (Araştırma Makalesi)	
Abayhan BURAN, Murat Ersin DURĞUN, Ercan AYDOĞMUŞ, Hasan ARSLANOĞLU	12
Detection of brain tumor with a pre-trained deep learning model based on feature selection using MR images (Research Article) MR görüntüleri kullanılarak öznelik seçimine dayalı ön-eğitilmiş bir derin öğrenme modeliyle beyin tümörünün tespiti (Araştırma Makalesi)	
Kürşat DEMİR, Berna ARI, Fatih DEMİR	23
An examination of synthetic images produced with DCGAN according to the size of data and epoch (Research Article) DCGAN ile üretilen sentetik görüntülerin veri boyutuna ve epoch sayısına göre incelenmesi (Araştırma Makalesi)	
Canan KOÇ, Fatih ÖZYURT	32
Investigation of flow properties and activation energy of magnesium lignosulfonate modified bitumen (Research Article) Magnezyum lignosülfonat modifiyeli bitümün akış özelliklerinin ve aktivasyon enerjisinin araştırılması (Araştırma Makalesi)	
Ahmet Münir ÖZDEMİR, Bahadır YILMAZ	38



Behaviour of a strip footing adjacent to the existing supported excavation

Mevcut destekli kazıya bitişik bir şerit temelin davranışı

Mesut GÖR^{1*}, Nichirvan Ramadhan TAHER², Hüseyin Suha AKSOY³

^{1,2,3}Department of Civil Engineering, Faculty of Engineering, Firat University, Elazig, Turkey.
¹mgor@firat.edu.tr, ²taher.nichirvan@gmail.com, ³saksoy@firat.edu.tr

Received: 23.11.2022
Accepted: 17.01.2023

Revision: 12.01.2023

doi: 10.5505/fujece.2023.13007
Research Article

Abstract

This study investigates the results of the numerical analysis on effect of existing supported excavation on ultimate bearing capacity (q_{ult}) of strip footing adjacent to supported excavation in sandy soil. The influence of distance (L) between the foundation and the supported excavation was studied as well as the effect of the excavation depth (H_e). For this purpose, on a full-scale model, a series of numerical calculations were carried out to determine how (L) and (H_e) affected the behavior of strip foundation. Based on finite element approach, the computer software Plaxis 2D code was utilized. Non-linear hardening soil model, a sophisticated elastoplastic stress-strain constitutive soil model, was used to characterize sandy soil. Based on Mindlin's beam theory, the strip footing and sheet pile wall were identified as elastic beam components with significant flexural rigidity (EI) and axial stiffness (EA). The sheet pile was installed at three different distances (L) away from the face of the strip foundation $1B$, $1.5B$ and $2B$, where B is the width of foundation. For each distance, three different excavations (H_e) were used with dimensions $1B$, $1.5B$ and $2B$. The numerical outcomes show that the ultimate bearing capacity (q_{ult}) of shallow foundation is decreased when distance between strip foundation and supported excavation is decreased, and vice versa. Additionally, (q_{ult}) is reduced as the depth of excavation behind sheet pile wall is increased, and vice versa.

Keywords: Finite element methods, Supported excavation, Strip foundation, Sheet pile, Excavation depth

Özet

Bu çalışmada, kumlu zeminde destekli bir kazıya bitişik olan bir şerit temelin nihai taşıma gücüne (q_{ult}) mevcut destekli kazı etkisinin sayısal olarak incelenmesi ve sonuçları araştırılmıştır. Şerit temelin taşıma gücü üzerinde, temel ile destekli kazı arasındaki mesafenin (L) etkisi ile kazı derinliğinin (H_e) etkisi incelenmiştir. Bu amaçla, tam ölçekli bir model üzerinde, (L) ve (H_e)'nin şerit temelin davranışını nasıl etkilediğini belirlemek için bir takım sayısal hesaplamalar yapılmıştır. Sayısal analizlerde sonlu elemanlar yaklaşımına dayalı olarak çalışan bir bilgisayar yazılımı olan Plaxis 2D paket programı kullanılmıştır. Kumlu zemini karakterize etmek için doğrusal olmayan sertleşen zemin modeli (söfistike bir elastoplastik gerilme-gerinim yapıcı zemin modeli) kullanılmıştır. Mindlin'in giriş teorisine dayanarak, şerit temel ve palplans duvar, önemli eğilme rijitliğine (EI) ve aksel rijitliğe (EA) sahip elastik giriş bileşenleri olarak tanımlanmıştır. Palplans, şerit temelin yüzünden, $1B$, $1.5B$ ve $2B$ olmak üzere üç farklı mesafede (L) yerleştirilmiş olup burada B temelin genişliğini göstermektedir. Her mesafe için $1B$, $1.5B$ ve $2B$ boyutlarında üç farklı kazı derinliği (H_e) kullanılmıştır. Sayısal sonuçlar, şerit temel ile desteklenen kazı arasındaki mesafe azaldıkça şerit temelin nihai taşıma kapasitesinin (q_{ult}) azaldığını ve arttıkça da bunun tersinin oluştuğunu göstermektedir. Ayrıca, duvarın arkasındaki kazı derinliği arttıkça taşıma gücünün (q_{ult}) azaldığı ve kazı derinliği azaldıkça taşıma gücünün arttığı sonucuna da varılmıştır.

Anahtar kelimeler: Sonlu elemanlar metodu, Destekli kazı, Şerit temel, Palplans, Kazı derinliği

1. Introduction

In constructing an excavation, controlling ground surface settlement near excavation area is an important duty. In a number of instances, it is recommended that buildings in metropolitan areas have basement construction or subsurface features like cut-and-cover tunnels excavated adjacent to them. The most dangerous constructions are those that are supported by shallow foundations that do not extend below the excavation's effect zone. When new structure's foundation excavation depth is larger than existing structure's foundation level, the excavation must be supported by

*Corresponding author

a retaining structure while new building's foundation is being built. It is extremely important to prevent or reduce damage to neighboring building by using different types of support structures [1]. The bearing capacity of strip foundation near supported excavation is influenced by numerous factors, such as stiffness of excavation support system, installation procedures of the system, soil conditions, distance of foundation from excavation, and size of the foundation. Excavation-related limiting requirement depends on shear strength parameters of soil, methods of excavation, building type, and type of ground support system [2]. Studying characteristics of shallow foundations near deep-supported excavation is a complicated geotechnical issue. Changes occur as soil is excavated behind the sheet pile wall or any retaining structures, such as state of stress in soil around the excavation and movement of soil, and these changes affect also buildings or any structure near the excavation [3]. The assessment of ground movements has attracted interest in several research due to significant impact that deep excavation has on ground movements on nearby buildings or structures. These studies have mostly concentrated on predicting lateral movement related to deep excavation and settlement of existing building foundations [4-11]. The work done by Peck [4] was expanded by Clough [5] and they proposed analytical settlement envelopes. Oue et al., [6] gathered and examined field data relating to wall displacement in connection with deep excavation, and characterized the obvious impact range for estimating damage to surrounding structures. Yoo [8] gathered field data from more than 60 various excavation sites on lateral wall movement for walls built in overlying rock soils and analyzed the data regarding walls and types of support. Leung and Ng [11] gathered and analyzed field monitoring data from the execution of 14 multi-supported deep excavations in various ground conditions on the lateral deflection of walls and settlement of ground surface. Recently, numerical modelling analysis based upon the finite element methods (FEM) has become very popular in the analysis and design of geotechnical structures such as tunnels, dams, slope stability, shallow and foundations [12-16]. Many researchers have used FEM also to study the effects of deep excavation on the existing nearby structures [17-21].

The purpose of this study is to investigate the effect of supported excavation on the bearing capacity of the adjacent strip foundation in sandy soil. The FEM code, PLAXIS 2D, was selected as the numerical tool, the studied factors were the distance (L) between the face of the shallow foundation and supported excavation and the depth of the excavation (H_e). For this purpose, sheet pile was installed at three different distances (L) away from the face of shallow foundation which is ($1B$, $1.5B$ and $2B$), where B is the width of the foundation. For each distance, three different excavation was used with dimensions ($1B$, $1.5B$ and $2B$).

2. Materials and Numerical Modelling

The hardening soil model was employed in this study to simulate the soil's nonlinear behavior. One of the most sophisticated soil models available, this constitutive model simulates many kinds of soil. Table 1 and 2 provides an overview of the material properties of sandy soil, sheet pile wall, and strip footing obtained from Plaxis 2D material model manual [22]. The strip footing and sheet pile wall were defined as elastic beam elements based on Mindlin's beam theory with important flexural rigidity (EI) and axial stiffness (EA). Since the full volume element method is slow from the point of view of computation time, therefore Mindlin's Beam Theory Constitutive Model was used as it reduces the computation time. Interface components are used to describe the interaction between sheet pile wall and soil on both sides, allowing for the specification of reduced wall friction relative to soil friction. This study investigates the bearing capacity of strip footing near supported excavation, the effect of distance (L) between strip footing and supported excavation and depth of excavation behind supported excavation (H_e) will be studied. For this purpose, a series of finite element analyses were done. Two-dimensional finite element method was used with 15-node plane strain model using Plaxis 2D computer program. The numerical analysis programs with various parameters are summarized in Figure 1. The impact of mesh dependency on the outcomes of the numerical analysis was minimized by using a fine enough mesh. The typical produced mesh for full-scale geometry and boundary conditions is shown in Figure 2. Model boundary conditions were assumed as follows; the vertical boundary is vertically deformable and laterally fixed while bottom boundary was meant to be certainly fixed. For groundwater conditions, it is assumed that water table is located deep below sand layer and therefore has no effect on the results of the analysis.

Table 1. Parameters of the sand used in FEM analysis [23]

Parameters	Value
Drainage type	Drained
Dry Unit Weight (γ_d) (kN/m ³)	17.0
E_{50}^{ref} ($P_{ref} = 100$ kPa) (kN/m ²)	43000
E_{ur}^{ref} ($P_{ref} = 100$ kPa) (kN/m ²)	129000
E_{oed}^{ref} ($P_{ref} = 100$ kPa) (kN/m ²)	22000
Cohesion, (c) (kN/m ²)	1.0
Friction angle, (ϕ) (°)	34.0
Dilatancy angle (ψ) (°)	4.0
Poisson's ratio (ν_{ur})	0.20
K_0^{nc}	0.34
m, Power	0.50
R_{inter}	0.70

Table 2. Parameters of the sheet pile wall and strip footing [23]

Parameters	Sheet pile	Strip footing
Material type	Elastic; Isotropic	Elastic; Isotropic
Flexural rigidity (EA), kN/m	$12 * 10^6$	$11.5 * 10^6$
Normal stiffness (EI), kN m ² /m	$12 * 10^4$	$2396 * 10^2$
Thickness (d), cm	35.0	50.0
Weight (w) kN/m/m	8.3	0
Poisson's ratio	0.15	0

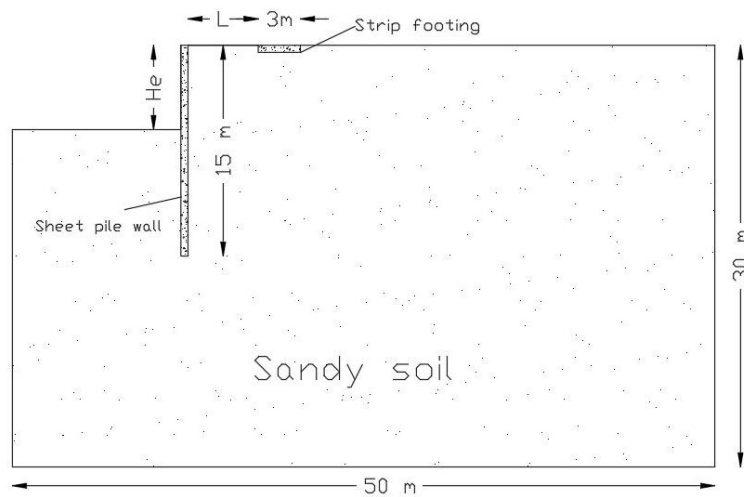


Figure 1. Geometric parameters studied in numerical analysis

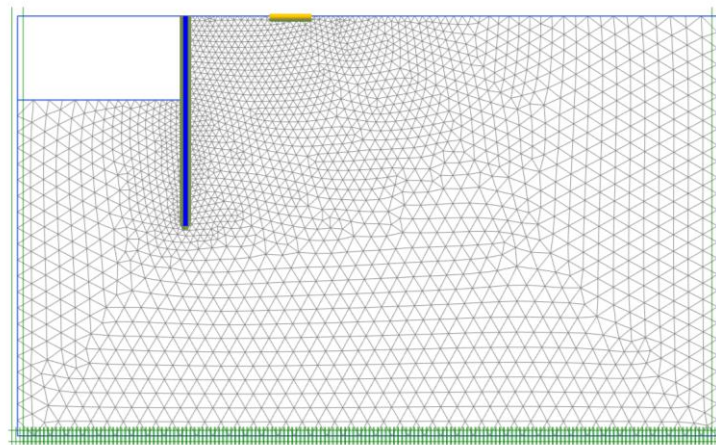


Figure 2. Typical generated mesh for prototype geometry

3. Results and Discussion

After performing numerical analysis to investigate the effects of distance (L) between shallow foundation and supported excavation by sheet pile wall. To this end, sheet pile was installed at three different distances (L) away from the face of the shallow foundation with dimensions ($1B$, $1.5B$ and $2B$). The sand behind sheet pile was excavated with dimensions ($1B$, $1.5B$ and $2B$) For each distance. This section discusses the findings from numerical analysis. Ultimate bearing capacity of strip footing was determined by applying prescribed line displacement on the footing. It is assumed that the strip footing reaches the settlement value of 25 mm and the required load corresponding to this settlement value is calculated. The settlement values of 25 mm are considered ultimate bearing capacity loads [24]. After performing FEM analysis, the results were obtained as load-vertical displacement and load-lateral displacement for shallow foundation and sheet pile wall, respectively. The typical deformation mesh of the soil, sheet pile wall displacement, and foundation displacement are shown in figure 3. Figures 4 through 9 show the load-vertical displacement curves of the foundation and load-lateral displacement sheet pile with different distances (L) and different excavation depths (H_e).

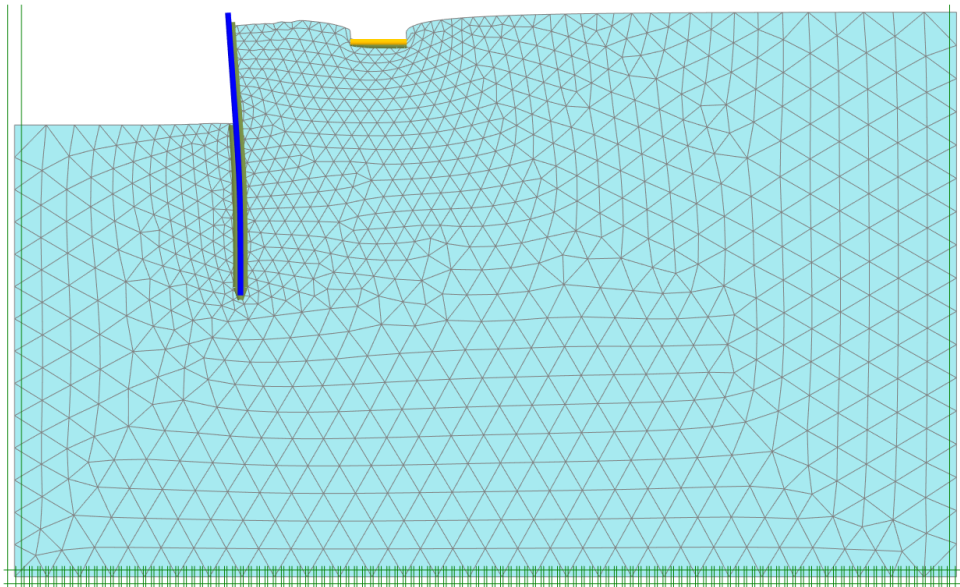


Figure 3. Deformed mesh (logarithmically scaled up 150 times)

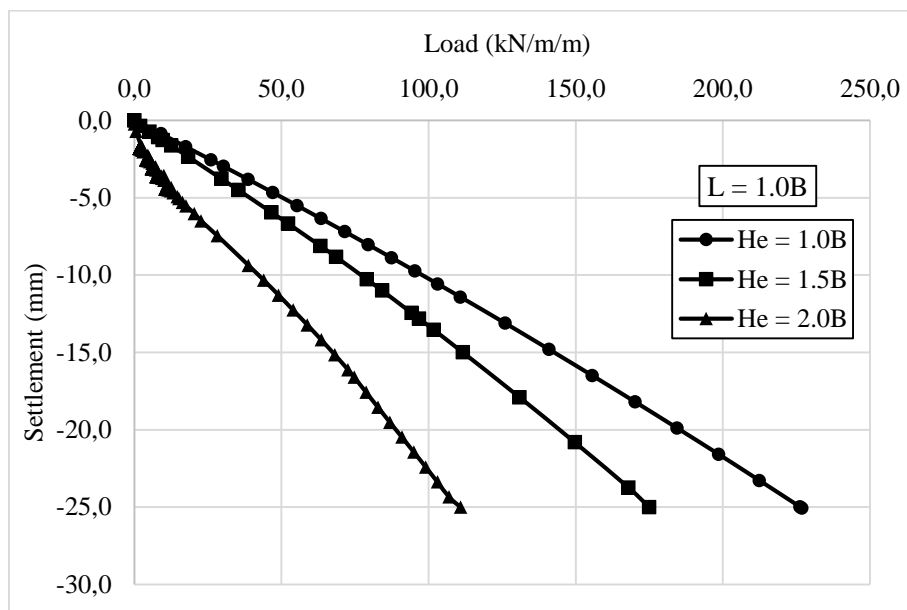


Figure 4. Load-vertical displacement curves for strip footing by 1.0B away from the supported excavation with different excavation depths (H_e)

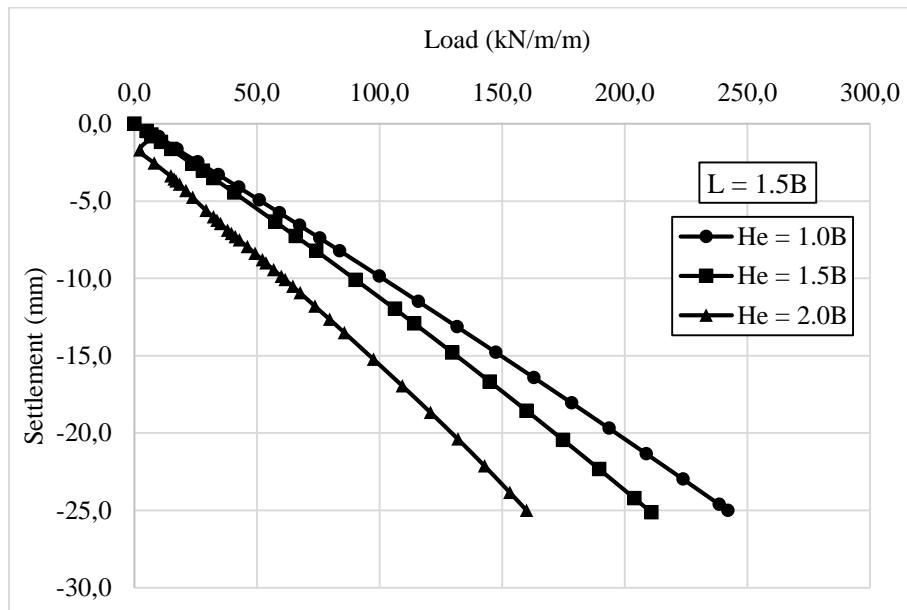


Figure 5. Load-vertical displacement curves for strip footing by 1.5B away from the supported excavation with different excavation depths (He)

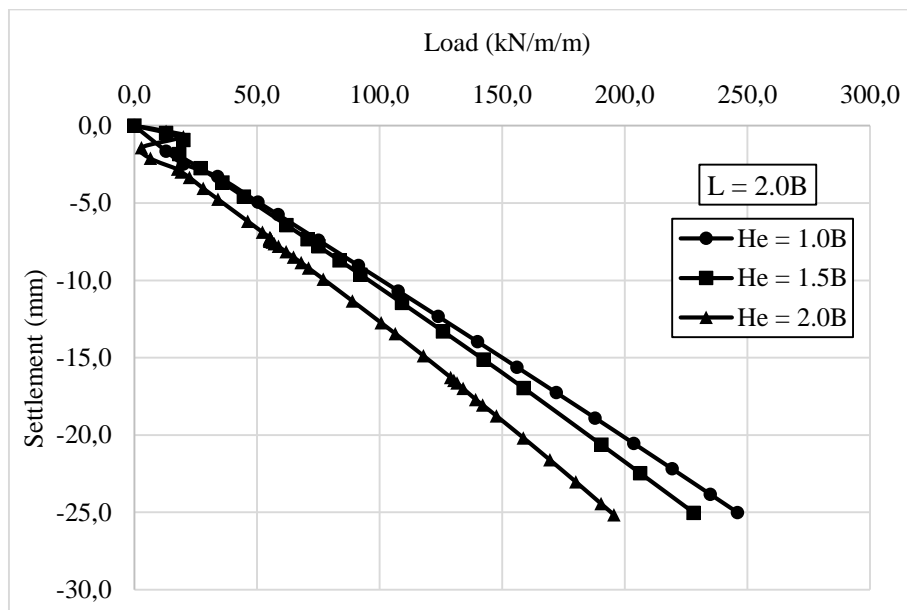


Figure 6. Load-vertical displacement curves for strip footing by 2.0B away from the supported excavation with different excavation depths (He)

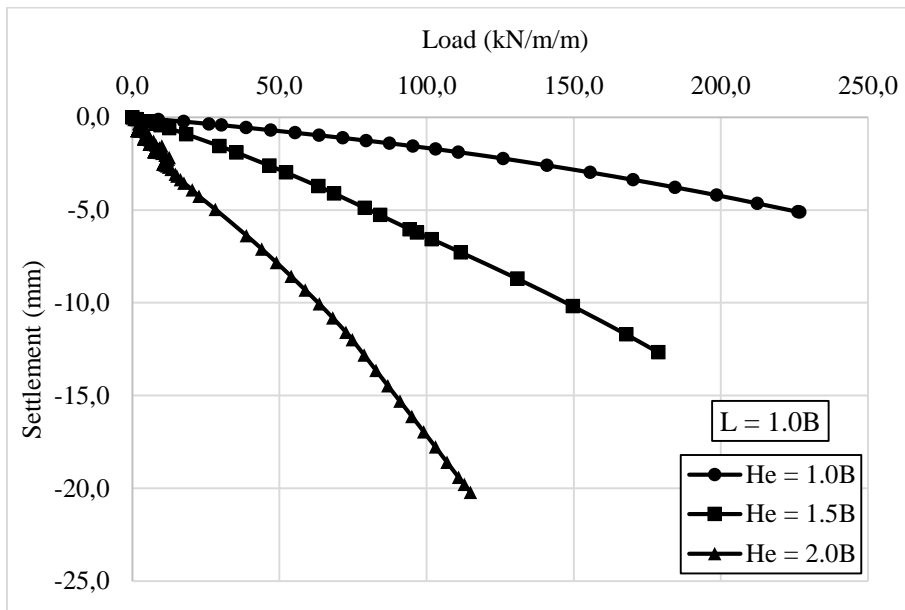


Figure 7. Load-lateral displacement curves for sheet pile by 1.0B away from the strip footing with different excavation depths (He)

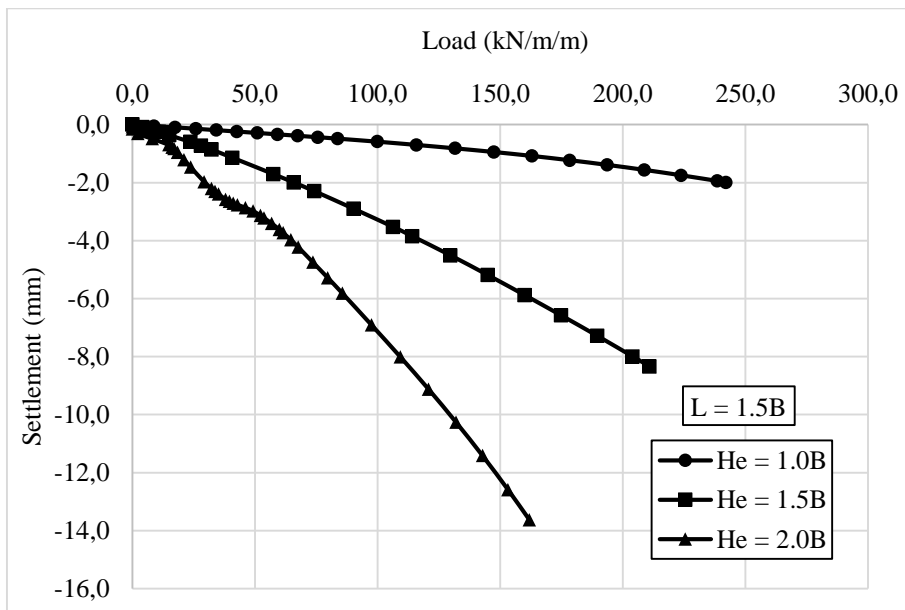


Figure 8. Load-lateral displacement curves for sheet pile by 1.5B away from the strip footing with different excavation depths (He)

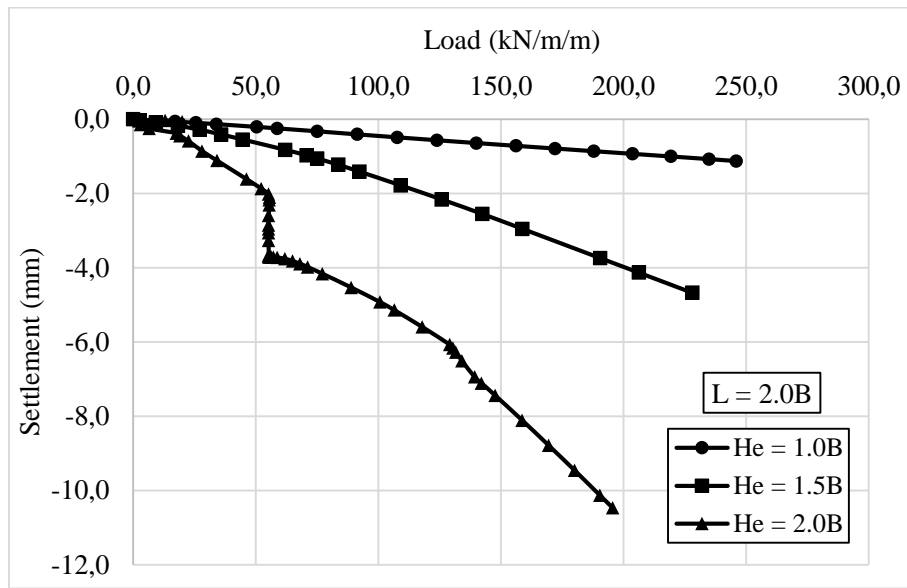


Figure 9. Load-lateral displacement curves for sheet pile by 2.0B away from the strip footing with different excavation depths (He)

The impact of existing supported excavation with different distances from strip footing and different excavation depths behind supported excavation on bearing capacity of foundation is presented in Figure 10. It can be seen that as the distance between strip footing and supported excavation increases, its bearing capacity increases, also, it is decreased with increasing excavation depth behind supported excavation. The change in lateral displacement at top of sheet pile with excavation depth/foundation width is shown in Figure 11. It is obvious the lateral displacement of sheet pile increases with increasing excavation depth/foundation width with different distances from the foundation. The variation of the maximum moment force of the sheet pile with different distances from the foundation and different excavation depths is illustrated in Figure 12. It is evident that the maximum moment of the sheet pile is observed when the supported excavation is 1.0B away from the foundation with an excavation depth equal to 2B. When the distance between supported excavation and foundation increases the maximum moment of the sheet pile decreases and vice versa.

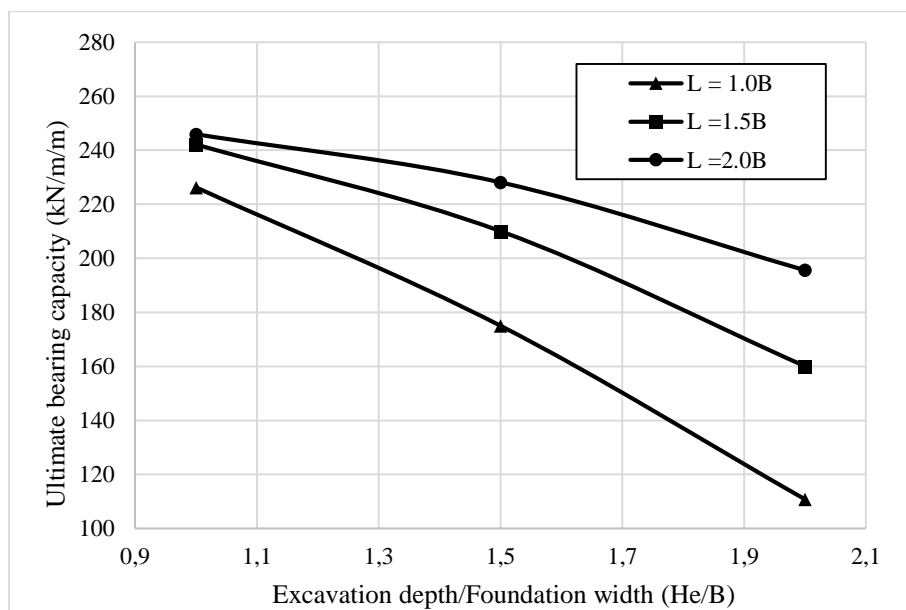


Figure 10. Change in the ultimate bearing capacity of the strip footing with (He/B)

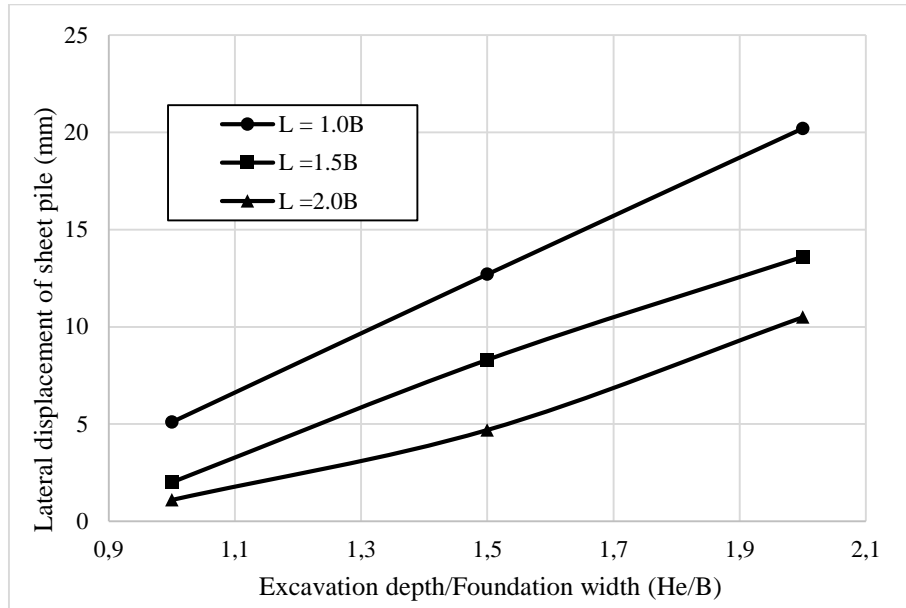


Figure 11. Variation of lateral displacement of the sheet versus (He/B)

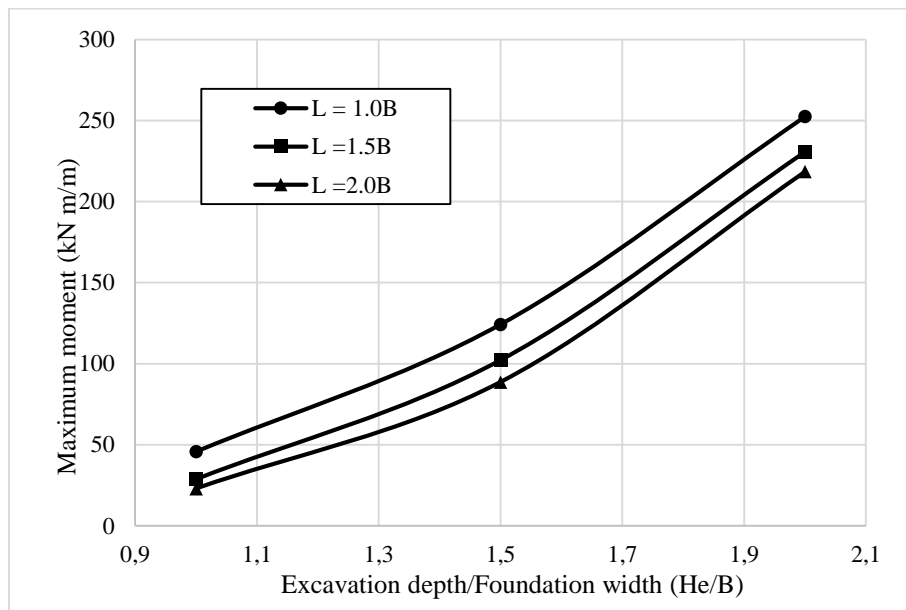


Figure 12. Variation of maximum moment of the sheet pile versus (He/B)

4. Conclusion

In this study, Plaxis 2D FEM code was used to numerically examine the impact of existing supported excavation on strip foundation's bearing capacity. The influence of different distances (L) between supported excavation and face of foundation and different excavation depths (H_e) was examined. The following inferences can be made in light of numerical analysis results:

- The ultimate bearing capacity of strip foundation nearby supported excavation is decreased as the distance between supported excavation and foundation increases and the excavation depth as well.

- The lateral displacement of sheet pile increases with decreasing distance (L) between supported excavation and sheet pile. When the (L) equals foundation width (1.0B), the sheet pile is exposed to a considerable displacement as excavation depth (He) increases, but When the (L) equals (2.0B) the increase of lateral displacement of sheet pile is small with increasing excavation depth (He).
- The maximum moment in sheet pile wall is increasing with decreasing the distance (L) between supported excavation and strip foundation and excavation depth behind sheet pile as well.

5. Acknowledgment

This section is optional. However, this section should not be left blank when the article is submitted for the first time. If the article is supported by any institution, project, person, etc., the relevant information can be specified in this section.

6. Author Contribution Statement

Mesut GÖR and Nichirvan Ramadhan TAHER: Methodology, Software, Data collection and/or processing, Data analysis and interpretation, Writing - original draft. Hüseyin Suha AKSOY: Literature search, Critical revision of manuscript, Writing – review & editing.

7. Ethics Committee Approval and Conflict of Interest

“There is no conflict of interest with any person/institution in the prepared article”

8. References





- [1] El Sawwaf M, Nazir AK. "The effect of deep excavation-induced lateral soil movements on the behavior of strip footing supported on reinforced sand". *Journal of Advanced Research*, 3(4), 337-344, 2012.
- [2] Boone SJ. "Ground-movement-related building damage". *Journal of geotechnical engineering*, 122(11), 886-896, 1996.
- [3] Yoo C, Lee D. "Deep excavation-induced ground surface movement characteristics—A numerical investigation". *Computers and Geotechnics*, 35(2), 231-252, 2008.
- [4] Peck RB. "Deep excavations and tunneling in soft ground". *Proc. 7th ICSMFE*, 1969, 225-290, 1969.
- [5] Clough GW. "Construction induced movements of in situ walls". *Design and Performance of Earth Retaining Structures*, 439-470, 1990.
- [6] Ou CY, Hsieh PG, Chiou DC. "Characteristics of ground surface settlement during excavation". *Canadian Geotechnical Journal*, 30(5), 758-767, 1993.
- [7] Long M. "Database for retaining wall and ground movements due to deep excavations". *Journal of Geotechnical and Geoenvironmental Engineering*, 127(3), 203-224, 2001.
- [8] Yoo C. "Behavior of braced and anchored walls in soils overlying rock". *Journal of Geotechnical and Geoenvironmental Engineering*, 127(3), 225-233, 2001.
- [9] Wang ZW, Ng CW, Liu GB. "Characteristics of wall deflections and ground surface settlements in Shanghai". *Canadian Geotechnical Journal*, 42(5), 1243-1254, 2005.
- [10] Liu G, Ng CW, Wang Z. "Observed performance of a deep multistrutted excavation in Shanghai soft clays". *Journal of Geotechnical and Geoenvironmental Engineering*, 131(8), 1004-1013, 2005.
- [11] Leung EH, Ng CW. "Wall and ground movements associated with deep excavations supported by cast in situ wall in mixed ground conditions". *Journal of Geotechnical and Geoenvironmental Engineering*, 133(2), 129-143, 2007.
- [12] Keskin İ. "An evaluation on effects of surface explosion on underground tunnel; availability of ABAQUS Finite element method". *Tunnelling and Underground Space Technology*, 120, 104306, 2022.
- [13] Awlla HA, Taher NR, Mawlood YI. "Effect of fixed-base and soil structure interaction on the dynamic responses of steel structures". *International Journal of Emerging Trends in Engineering Research*, 8(9), 2020.
- [14] Taher N R, Gör M, Aksoy HS, Ahmed H. "Numerical investigation of the effect of slope angle and height on the stability of a slope composed of sandy soil". *Gümüşhane Üniversitesi Fen Bilimleri Dergisi*, 12(2), 664-675, 2022.

- [15] Awlla HA, Taher NR, AKSOY HS, Qadir AJ. "Effect of SSI and fixed-base concept on the dynamic responses of Masonry Bridge structures, Dalal Bridge as a case study". *Academic Journal of Nawroz University*, 11(3), 89-99, 2022.
- [16] Gör M, et al. *Effect of geogrid inclusion on the slope stability*. in *Proceedings of the V-International European Conference on Interdisciplinary Scientific Research, Valencia, Spain*. 2022.
- [17] Houhou MN, Emeriault F, Belounar A. "Three-dimensional numerical back-analysis of a monitored deep excavation retained by strutted diaphragm walls". *Tunnelling and Underground Space Technology*, 83, 153-164, 2019.
- [18] Likitlersuang S. et al. "Finite element analysis of a deep excavation: A case study from the Bangkok MRT". *Soils and Foundations*, 53(5), 756-773, 2013.
- [19] Lim A, Ou CY, Hsieh PG. "A novel strut-free retaining wall system for deep excavation in soft clay: numerical study". *Acta Geotechnica*, 15(6), 1557-1576, 2020.
- [20] Zhao W, et al. "A numerical study on the influence of anchorage failure for a deep excavation retained by anchored pile walls". *Advances in Mechanical Engineering*, 10(2), 1687814018756775, 2018.
- [21] Cui HH, Zhang L, Zhao GJ. "Numerical simulation of deep foundation pit excavation with double-row piles". *Rock and Soil Mechanics-Wuhan*, 27(4), 662, 2006.
- [22] Abeje W. *Soil Stabilization using plastic wastes (Case Study on Addis Ababa)*. 2017.
- [23] Brinkgreve R. et al. "PLAXIS 2016". PLAXIS bv, the Netherlands, 2016.
- [24] Bowles JE. "Foundation Analysis and Design, The McGrawHill Companies". Inc., Singapore, 1996.



Determination of thermophysical properties of *Ficus elastica* leaves reinforced epoxy composite

Kauçuk ağacı (*Ficus elastica*) yaprağı takviyeli epoksi kompozitin termofiziksel özelliklerinin belirlenmesi

Abayhan BURAN¹ , Murat Ersin DURĞUN² , Ercan AYDOĞMUŞ³ , Hasan ARSLANOĞLU^{4*} 

^{1,2}Department of Bioengineering, Faculty of Engineering, Firat University, Elazığ, Turkey.

³Department of Chemical Engineering, Faculty of Engineering, Firat University, Elazığ, Turkey.

⁴Department of Chemical Engineering, Faculty of Engineering, Canakkale Onsekiz Mart University, Canakkale, Turkey.

¹a.buran@firat.edu.tr, ²medurgun@firat.edu.tr, ³ercanaydogmus@firat.edu.tr, ⁴hasan.arslanoglu@comu.edu.tr

Received: 19.01.2023
Accepted: 30.01.2023

Revision: 25.01.2023

doi: 10.5505/fujece.2023.21931
Research Article

Abstract

In this study, *Ficus elastica* leaves have been reinforced into an epoxy composite and some physical and chemical characterization of the obtained composite is made. *Ficus elastica* leaves are ground between 297 and 149 microns. The biomass (*Ficus elastica*) prepared as a filler material is kept in sodium hydroxide (% 7 NaOH) solution for 24 hours for alkali activation. It is then washed three times with distilled water and dried in an oven at 75 °C for 3 hours. Composite production is carried out by reinforcing the prepared filler to the epoxy resin in certain proportions by mass. The effect of the biomass filler added at the rate of 0 wt.%, 1 wt.%, 3 wt.%, 5 wt.%, and 7 wt.% on the density, Shore D hardness, thermal conductivity coefficient, and activation energy of the epoxy composite is determined. According to the results obtained, the density of the epoxy composite decreases as the filler ratio in the mixture increases. Shore D hardness of epoxy composite decreases with the addition of biomass filler. The epoxy composite produced with biomass reinforcement reduces both the thermal conductivity coefficient and the activation energy. Besides, when the chemical bond structure of the obtained polyester composite is analyzed by Fourier transform infrared spectrometer (FTIR), it is seen that there is a physical interaction. According to scanning electron microscopy (SEM) images, 5 wt.% and 7 wt.% reinforcement of *Ficus elastica* leaves negatively affects the surface morphology of the epoxy composite.

Keywords: Epoxy composite, *Ficus elastica*, Density, Shore D hardness, Thermal conductivity coefficient, Activation energy

Özet

Bu çalışmada, *Ficus elastika* yaprakları takviye edilerek epoksi kompozit üretilmekte ve elde edilen kompozitin bazı fiziksel ve kimyasal özellikleri karakterize edilmektedir. *Ficus elastika* yaprakları 297 ile 149 mikron arasında öğütülmektedir. Dolgu maddesi olarak hazırlanan biyokütle (*Ficus elastika*) alkali aktivasyonu için % 7'lik sodyum hidroksit (NaOH) çözeltisinde 24 saat bekletilmektedir. Daha sonra distile su ile 3 kez yıkanmakta ve 75 °C sıcaklıkta etüvde 3 saat kurutulmaktadır. Kompozit üretimi, hazırlanan dolgu maddesinin epoksi reçineye kütlece belirli oranlarda takviye edilmesiyle gerçekleştirilmektedir. Ağırlıkça % 0, % 1, % 3, % 5 ve % 7 oranlarında eklenen biyokütle dolgu maddesinin yoğunluk, Shore D sertlik, ısıl iletkenlik katsayısı ve aktivasyon enerjisi üzerine etkisi epoksi kompozitte belirlenmektedir. Elde edilen sonuçlara göre karışımdaki dolgu oranı arttıkça epoksi kompozitin yoğunluğu azalmaktadır. Epoksi kompozitin Shore D sertliği, biyokütle dolgu maddesi ilavesiyle azalmaktadır. Biyokütle takviyesi ile üretilen epoksi kompozitin hem ısıl iletkenlik katsayısı hem de aktivasyon enerjisini düşürmektedir. Ayrıca elde edilen polyester kompozitin kimyasal bağ yapısı Fourier dönüşümlü kızılötesi spektrometre (FTIR) ile incelendiğinde fiziksel bir etkileşimin gerçekleştiği görülmektedir. Taramalı elektron mikroskobu (SEM) görüntülerine göre, *Ficus elastika* yapraklarının ağırlıkça % 5 ve % 7 takviyesi, epoksi kompozitin yüzey morfolojisini olumsuz etkilemektedir.

Anahtar kelimeler: Epoksi kompozit, *Ficus elastica*, Yoğunluk, Shore D sertlik, Isıl iletkenlik katsayısı, Aktivasyon enerjisi

*Corresponding author

1. Introduction

Today, the use of bioresources in the production of pure polymers and composites is becoming more and more common. Especially environmentally friendly, economical, and some mechanical properties improved polymers are preferred. For example, inorganic industrial wastes are used to increase thermal stability in the production of polymers such as polyester and epoxy. After the boron factory components and wastes are ground very finely, they are reinforced in polymers as filler. Thus, the density, hardness, and thermal stability of the polymer composite are increased. Improvements are also observed in mechanical properties when used at optimum rates [1-4].

In the literature, inorganic fillers such as colemanite, ulexite, tincal, and borax are used as fillers to obtain polyester and epoxy composites. To work at optimum ratios in the production of composites, such fillers are used in the range of 0 wt.% to 15 wt.%. The addition of 10 wt.% or more inorganic filler negatively affects both the surface morphology and the pore structure of the produced composite. It also increases the coefficient of thermal conductivity, density, and Shore D hardness. Therefore, optimum ratios (usually between 3 wt.% and 6 wt.%) of inorganic filler can be used in the polymer composite [5-9].

Besides, clay, diatomite, pumice, perlite, micro-glass spheres, and nanoparticles are used in the production of composites. To reduce the density of polyester and epoxy composites, low-density inorganic fillers are used. To improve mechanical properties, fillers such as alumina, graphene, carbon nanotube, silicon carbide, and multi-walled carbon nanotubes are preferred in polymer composites. Porous fillers such as pumice and perlite are used to increase the porosity of the composite material [10-18].

There are also studies in the literature on the reuse of industrial polymer wastes in polymer composites. For example, polymer wastes such as polyethylene terephthalate, tire rubber, cable, polyethylene, mask, and polyurethane can be used in composite production. In this way, both economical composite production is realized and polymer wastes that cause environmental pollution are eliminated [19-26].

Many composites are being improved, especially by reinforcing biomass wastes into polymers. Especially plants with a fibrous structure are involved in the production of composites such as polyester and epoxy composite components. Biomass wastes such as sunflower stalk, apricot stone shell, corncob, *Cornus alba*, and *Asphodelus aestivus* have been reinforced into polymer composite [27-32]. The fibrous structure, elastic property, density, economy, workability, and compatibility of biomass wastes are very important. The leaves of rubber trees can be given as an example of the biomass wastes to be used in the study. Rubber trees, whose Latin name is *Ficus elastica*, are used as natural polymers in many sectors. *Ficus elastica* is an ornamental plant originating from tropical Asia. The plant is morphologically shiny and has a thick epicuticular wax layer on the green leaf surface [33-38].

The original direction of this research is the reinforcement of leaves of *Ficus elastica* as filler in the epoxy composite. In this study, biomass is used as a filler to obtain economical, environmentally friendly, and low-density composite materials. Epoxy composite with both low density and low thermal conductivity coefficient has been obtained. Biomass reinforcement at optimum rates (3 wt.%) does not negatively affect the porosity and surface morphology of the composite.

2. Materials and Methods

2.1. Materials

The epoxy resin components used in this study are supplied by Polisan Company. The leaves taken from the rubber ornamental plant (*Ficus elastica*) are prepared for epoxy composite production. Sodium hydroxide (Merck NaOH) is used for alkali activation. Figure 1 shows the dried leaves of *Ficus elastica*.



Figure 1. Dried Ficus elastica leaves

2.2. Methods

Biomass is reinforced in Epoxy A as filler at 0 wt.%, 1 wt.%, 3 wt.%, 5 wt.%, and 7 wt.% ratios. *Ficus elastica* leaves prepared in certain proportions are added to the resin, which is heated from room temperature to 55 °C. After providing a homogeneous mixing at 750 rpm and 5 min, Epoxy B is added to the mixture, mixed for 2 min, and cast into standard molds. After the curing process (24 hours) of the obtained epoxy composite is done, the necessary physical and chemical tests are carried out. The properties of the composite are determined by FTIR, SEM, density, Shore D hardness, thermal conductivity coefficient, and thermal stability tests [39-41]. Table 1 shows the amounts of components used in the epoxy composite production process. In Figure 2, the production scheme for the biomass reinforced epoxy composite is briefly shown.

Table 1. Epoxy composite preparation plan

Epoxy A (g)	Epoxy B (g)	Filler (g)
6.6	3.4	0.0
6.5	3.4	0.1
6.3	3.4	0.3
6.1	3.4	0.5
5.9	3.4	0.7

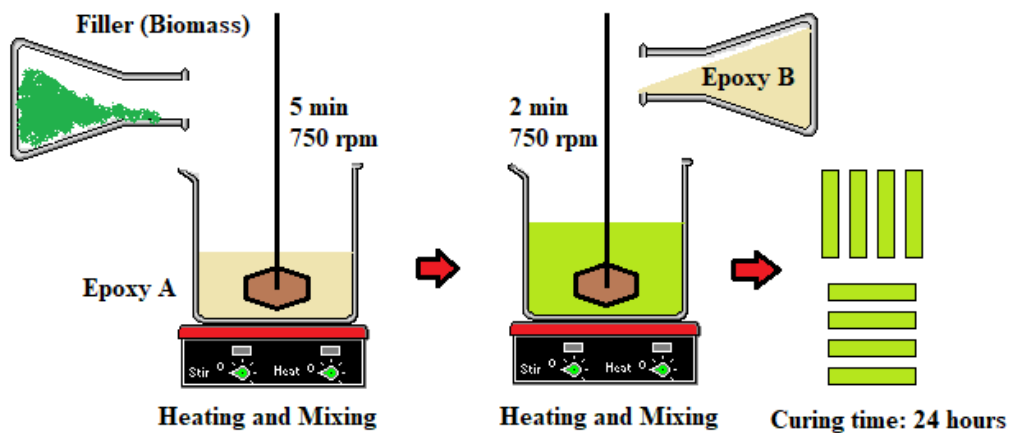


Figure 2. Biomass reinforced epoxy composite production scheme

3. Results and Discussions

3.1. Densities of the epoxy composites

Since the volume occupied by the obtained epoxy composites in standard molds is known, the matrix density is calculated from the mass/volume ratio. As expressed in Figure 3, the density of the epoxy composite decreases with biomass reinforcement. Biomass reinforcement reduces the density of the epoxy composite from 1134 kg/m³ to 1106 kg/m³.

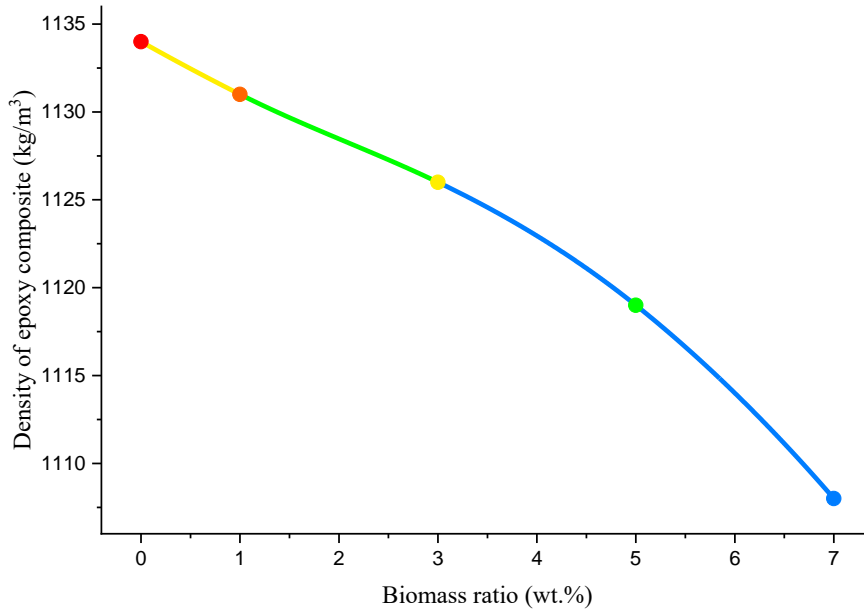


Figure 3. Effect of biomass reinforcement on the density of epoxy composite

3.2. Shore D hardness of the composites

The variation of Shore D hardness values of biomass reinforced epoxy composite with filler ratio is expressed in Figure 4. As seen in this figure, the biomass filler reinforced with epoxy reduces Shore D hardness of the composites. While the hardness value measured in the pure epoxy polymer is 77.5 Shore D, the hardness of 7 wt.% filler reinforced composite decreases to 75.6. *Ficus elastica* leaves can be said to reduce the hardness of the epoxy composite and increase its workability.

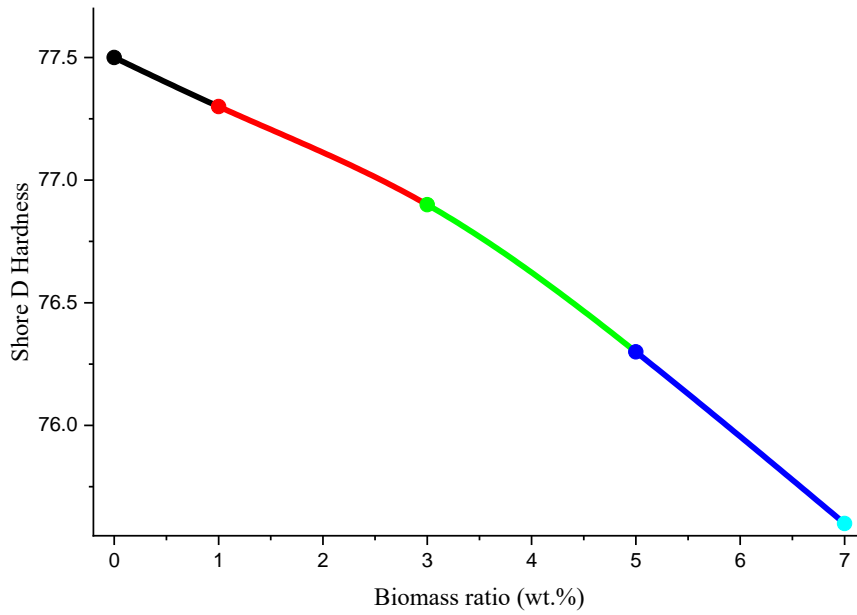


Figure 4. Change of hardness of epoxy composite with reinforcement of *Ficus elastica* leaves

3.3. Thermal conductivity coefficient of the epoxy composites

It has been determined that the thermal conductivity coefficient of the epoxy composite obtained by reinforcing *Ficus elastica* leaves decreases. In Figure 5, the thermal conductivity coefficient of the epoxy polymer is about 0.112 W/m·K, while it drops to 0.092 W/m·K with biomass supplementation.

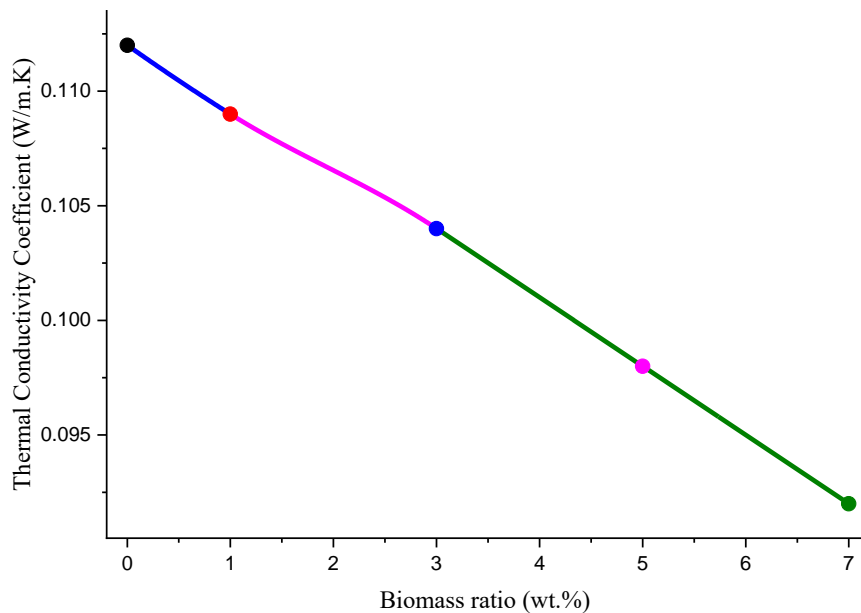


Figure 5. Effect of *Ficus elastica* leaves reinforcement on thermal conductivity of epoxy composite

3.4. Activation energy of the epoxy composites

In this section, the thermal stability of epoxy composites has been evaluated by calculating their activation energies. Weight loss of composites has been measured with temperature increase in an inert environment in a PID (proportional integral derivative) controlled experiment system. Activation energy (E_a) values are calculated

according to Coats-Redfern method. In this method, the highest correlation coefficients ($R^2 > 0.9895$) are found with the three-dimensional diffusion equation. The activation energies (conversion rate (α): 0.15-0.85) of biomass reinforced epoxy composites are calculated from room temperature to 600 °C with a temperature rise rate of about 10 °C/min. *Ficus elastica* leaves are found to decrease the activation energy values of the epoxy composite. In thermal decomposition experiments, physical impurities are removed from the samples in the range of about 25 °C to 150 °C. After a temperature of about 200 °C, the chemical decomposition region of the epoxy composite begins. It refers to the region where chemical decomposition occurs rapidly in the temperature range of 300 °C to 400 °C. Chemical decomposition appears to slow down in the temperature range of 450 °C to 600 °C. Figure 6 shows the variation of the activation energy of the epoxy composite with the biomass reinforcement ratio [42,43].

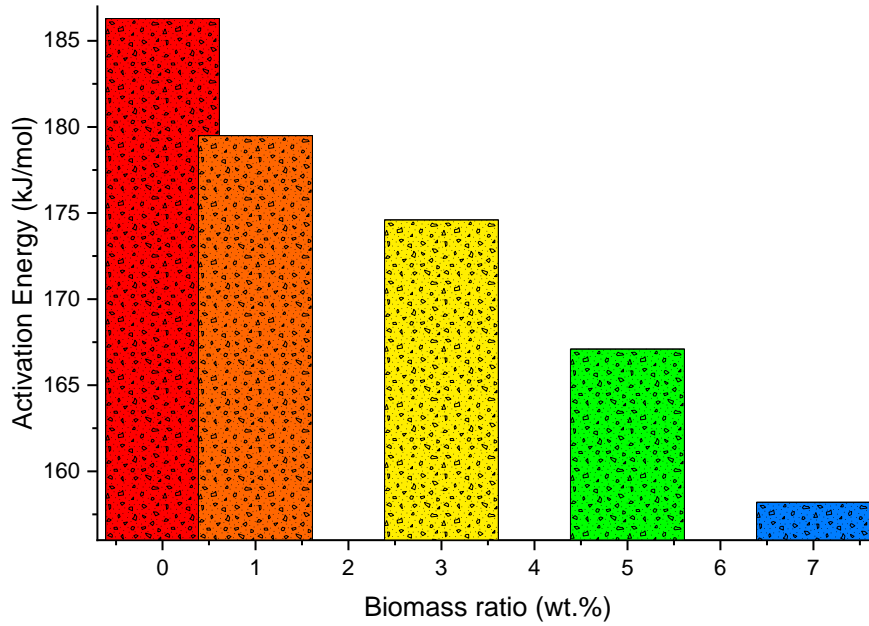


Figure 6. Change of activation energy of epoxy composite with biomass reinforcement

3.4. FTIR spectra of the epoxy composite

In this research, *Ficus elastica* leaves are used as filler in the epoxy composite. According to FTIR spectra results, there is no chemical bond between the biomass and the epoxy resin, but there is a physical interaction. When the FTIR spectra in Figure 7 are examined, C=O stretching vibrations of the ester groups are seen at a wavelength of 1715-1730 cm^{-1} , and a wavelength of 2850-3000 cm^{-1} attributed to the aliphatic C-H stretching band. It indicates the presence of the peak hydroxyl (OH) group seen at a wavelength of 3450 – 3550 cm^{-1} .

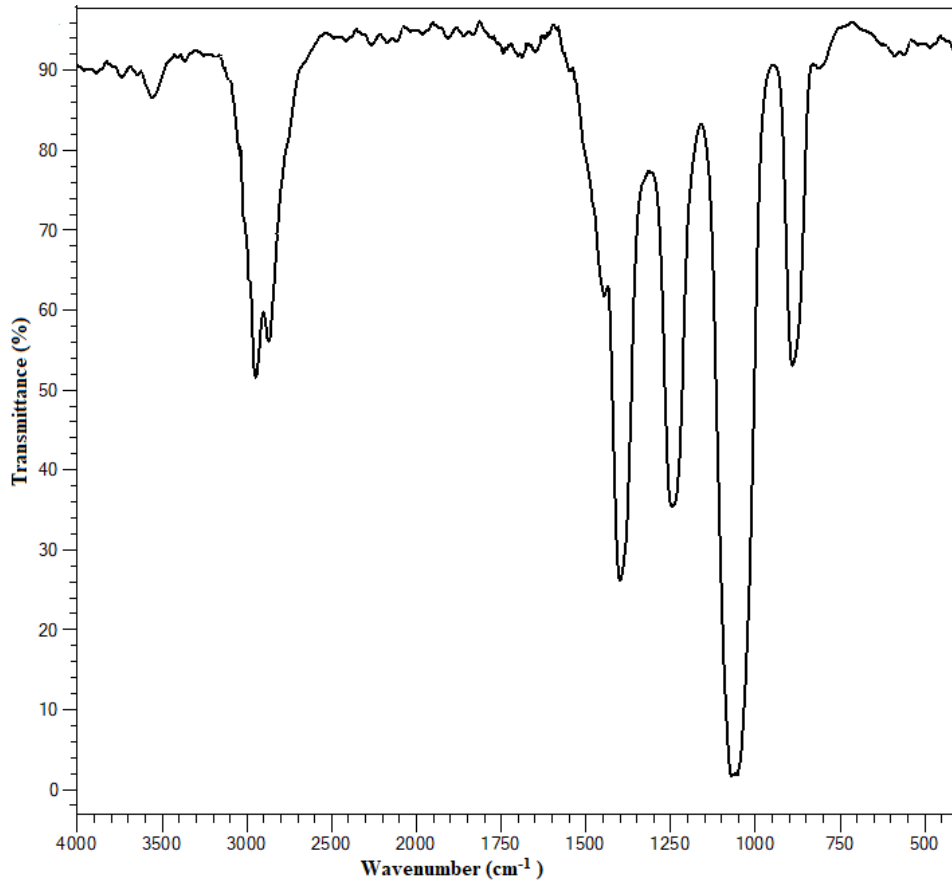


Figure 7. FTIR spectra of biomass (3 wt.%) reinforced epoxy composite

3.5. SEM image of the epoxy composite

In Figure 8, SEM image of the composite is given when the leaves of *Ficus elastica* plant are reinforced into epoxy resin at a rate of 1 wt.%. In Figure 9, it is seen that the high ratio of biomass reinforcement (7 wt.%) has a negative effect on the surface morphology of the epoxy composite and creates an irregular pore structure.

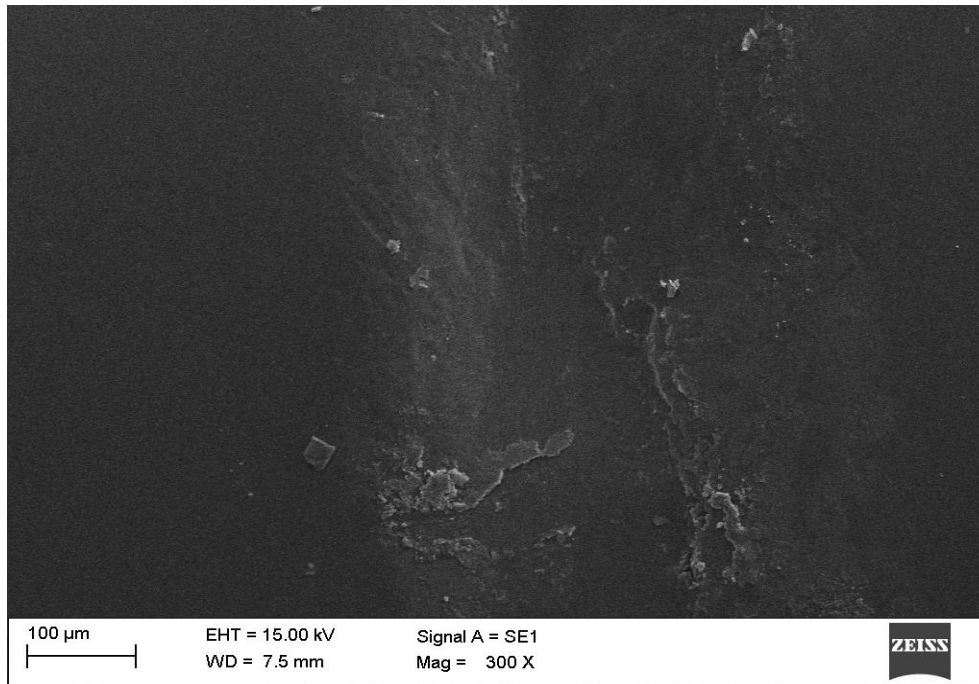


Figure 8. SEM image of epoxy composite reinforced with leaves of *Ficus elastica* (1 wt.%)

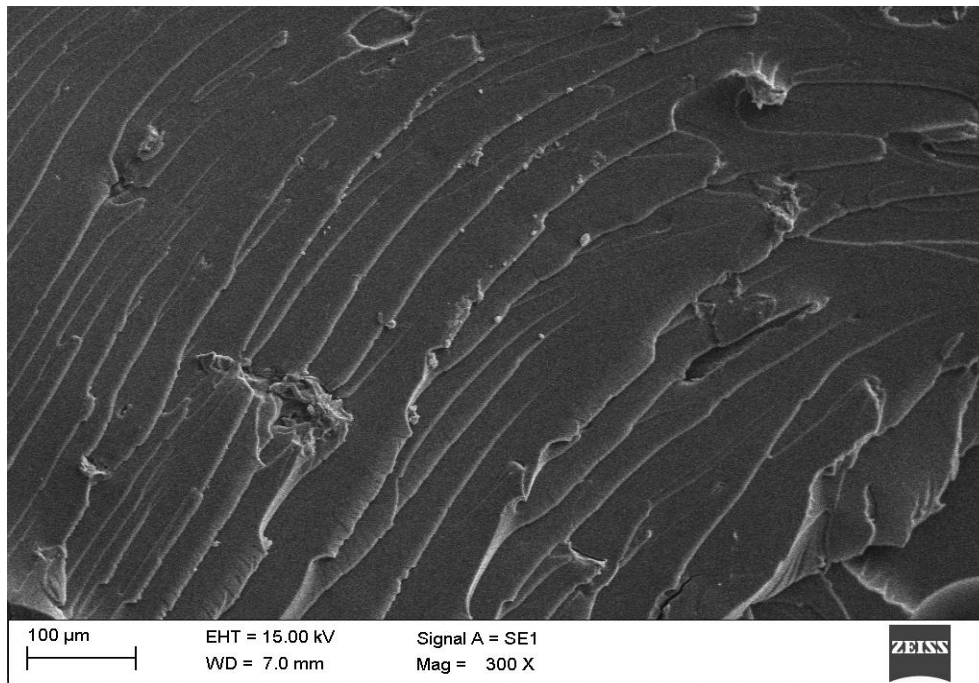


Figure 9. SEM image of epoxy composite reinforced with leaves of *Ficus elastica* (7 wt.%)

4. Conclusions

In this research, economical epoxy composites are produced from renewable resources by using biomass (*Ficus elastica* leaves). Both environmentally friendly and low carbon footprint composites are being improved. In this study, 0 wt.% 1 wt.%, 3 wt.%, 5 wt.%, and 7 wt.% biomass is reinforced into epoxy resin as filler. The thermal conductivity coefficient, activation energy, density, Shore D hardness, surface morphology, and chemical bond structure of the produced epoxy composites have been evaluated. According to the results obtained, biomass

reinforcement reduces the density of the epoxy composite. It is seen that the thermal conductivity coefficient of the composite decreases as the filler ratio increases in the epoxy resin. Since biomass reinforcement reduces the activation energy of the epoxy composite, it also reduces its thermal stability. Also, biomass reinforcement reduces Shore D hardness of the epoxy composite. The surface morphology and pore structure of the epoxy composite obtained with the optimum rate (3 wt.%) biomass reinforcement are not negatively affected.

5. Acknowledgments

We would like to thank Fırat University and Çanakkale Onsekiz Mart University for their contribution to the experimental studies in this research.

6. Author Contribution Statement

Murat Ersin DURĐUN and Abayhan BURAN contributed to making the design, and the literature review contributed to forming the idea, and the analysis of the results. Hasan ARSLANOĐLU and Ercan AYDOĐMUŞ contributed to conducting experimental studies, writing the article checking the spelling, and checking in terms of content.

7. Ethics Committee Approval and Conflict of Interest

There is no need for an ethics committee approval in the prepared article. There is no conflict of interest with any person/institution in the prepared article.

8. References




- [1] Dađ M, Yanen C, Aydođmuş E. "Effect of Boron Factory Components on Thermophysical Properties of Epoxy Composite". *European Journal of Science and Technology*, 36, 151–154, 2022.
- [2] Yılmaz E, Aydođmuş E, Demir A. "Life Cycle Assessment and Characterization of Tincal Ore Reinforced Polyester and Vinylester Composites". *Journal of the Turkish Chemical Society Section B: Chemical Engineering*, 5(2), 183-194, 2022
- [3] Yanen C, Dađ M, Aydođmuş E. "Investigation of Thermophysical Properties of Colemanite, Ulexite, and Tincal Reinforced Polyester Composites". *European Journal of Science and Technology*, 36, 155–159, 2022.
- [4] Aydođmuş E, Dađ M, Yalçın ZG. "Production and Characterization of The Composite from Unsaturated Polyester Resin with Tincal Ore". *4th International Conference on Physical Chemistry and Functional Materials*, Elazığ, 2021.
- [5] Yılmaz E, Aydođmuş E. "Production of Tincal Ore Reinforced Polyester Composite and Determination of Some Thermophysical Properties". *5th International Symposium on Innovative Approaches in Smart Technologies*, Türkiye, 2022.
- [6] Yılmaz E, Aydođmuş E, Demir A. "Production of Tincal Ore Reinforced Vinylester Composite and Investigation of Its Thermophysical Properties". *Karadeniz 9th International Conference on Applied Sciences*, Artvin, 2022.
- [7] Aydođmuş E, Dađ M, Yalçın ZG. "Thermal Decomposition Kinetics of the Colemanite Filled Polyester Composite". *3rd International Conference on Physical Chemistry and Functional Materials*, Malatya, 2020.
- [8] Aydođmuş E, Dađ M, Yalçın ZG. "Thermal Decomposition Kinetics of the Ulexite-Filled Polyester Composite". *3rd International Conference on Physical Chemistry and Functional Materials*, Malatya, 2020.
- [9] Orhan R, Aydođmuş E, Topuz S, Arslanođlu H. "Investigation of thermo-mechanical characteristics of borax reinforced polyester composites". *Journal of Building Engineering*, 42, 103051, 2021.
- [10] Aydođmuş E, Dađ M, Yalçın ZG. "Thermal Decomposition Kinetics of the Waste Clay Filled Polyester Composite". *3rd International Conference on Physical Chemistry and Functional Materials*, Malatya, 2020.
- [11] Dađ M, Yalçın ZG, Aydođmuş E. "Production of Diatomite Reinforced Polyester Composite and Investigation of Its Thermophysical Properties". *1st International Karatekin Science and Technology Conference*, Çankırı, 2022.

- [12] Dađ M, Aydođmuş E, Yalçın ZG. “Obtaining Diatomite Reinforced Epoxy Composite and Determination of Its Thermophysical Properties”. *1st International Karatekin Science and Technology Conference*, Çankırı, 2022.
- [13] Erzen B, Aydođmuş E. “Pumice Stone Reinforced Polyester Composite Production and Characterization”. *International Pumice and Perlite Symposium*, Bitlis, 2021.
- [14] Arslanođlu H, Aydođmuş E, Dađ M. “Obtaining and Characterization of Perlite Reinforced Epoxy Composites”. *International Pumice and Perlite Symposium*, Bitlis, 2021.
- [15] Aydođmuş E, Aydın M, Arslanođlu H. “Production and characterization of microsphere reinforced polyester composite: Modeling of thermal decomposition with ANN and optimization studies by RSM”. *Petroleum Science and Technology*, 1-17, 2022.
- [16] Şahal H, Aydođmuş E. “Investigation of Thermophysical Properties of Polyester Composites Produced with Synthesized MSG and Nano-Alumina”. *European Journal of Science and Technology*, 34, 95-99, 2022.
- [17] Şahal H, Aydođmuş E, Arslanođlu H. “Investigation of thermophysical properties of synthesized SA and nano-alumina reinforced polyester composites”. *Petroleum Science and Technology*, 1–17, 2022.
- [18] Yanen C, Aydođmuş E. “Characterization of Thermo-Physical Properties of Nanoparticle Reinforced the Polyester Nanocomposite”. *Dicle University Journal of the Institute of Natural and Applied Science*, 10(2), 121–132, 2021.
- [19] Aydođmuş E, Arslanođlu H, Dađ M. “Production of waste polyethylene terephthalate reinforced biocomposite with RSM design and evaluation of thermophysical properties by ANN”. *Journal of Building Engineering*, 44, 103337, 2021.
- [20] Aydođmuş E, Demirel MH. “Waste Tire Rubber Reinforced Polyester Composite Production and Characterization”. *8th International Conference on Materials Science and Nanotechnology for Next Generation*, Elazığ, 2021.
- [21] Arslanođlu H, Aydođmuş E. “WPET Reinforced Polyester Composite Production and Thermal Characterization by RSM Design”. *8th International Conference on Materials Science and Nanotechnology for Next Generation*, Elazığ, 2021.
- [22] Aydođmuş E, Dađ M, Yalçın ZG. “Obtaining of Some Industrial Factory Wastes Reinforced Polyester Composites”. *5th International Congress on Engineering and Technology Management*, İstanbul, 2021.
- [23] Aydođmuş E, Dađ M, Yalçın ZG “Thermal and Mechanical Properties of The Polyester Composites Produced with Cable Factory Wastes”. *4th International Conference on Physical Chemistry and Functional Materials*, Elazığ, 2021.
- [24] Aydođmuş E, Dađ M, Yalçın ZG, Arslanođlu H. “Synthesis and characterization of waste polyethylene reinforced modified castor oil-based polyester biocomposite”. *Journal of Applied Polymer Science*, 139, e525256, 2022.
- [25] Demirel MH, Aydođmuş E. “Production and Characterization of Waste Mask Reinforced Polyester Composite”. *Journal of Inonu University Health Services Vocational School*, 10(1), 41-49, 2022.
- [26] Demirel MH, Aydođmuş E. “Waste Polyurethane Reinforced Polyester Composite, Production and Characterization”. *Journal of the Turkish Chemical Society Section A: Chemistry*, 9(1), 443–452, 2022.
- [27] Orhan R, Aydođmuş E. “Production of Sunflower Stalk Reinforced Polyester Composite and Investigation of some Thermophysical Properties”. *Al-Farabi 4th International Congress on Applied Sciences*, Erzurum, 2022.
- [28] Orhan R, Topuz S, Aydođmuş E. “Experimental and Theoretical Study on Mechanical Properties of Apricot Stone Shell Reinforced Polyester Composites”. *3. Asia Pacific International Congress on Contemporary Studies*, South Korea, 2020.
- [29] Orhan R, Aydođmuş E. “Production and Characterization of Waste Corncob Reinforced Polyester Composite”. *European Journal of Science and Technology Special Issue*, 42, 176-179, 2022.
- [30] Buran A, Durğun ME, Aydođmuş E. “*Cornus alba* Reinforced Polyester-Epoxy Hybrid Composite Production and Characterization”. *European Journal of Science and Technology Special Issue*, (43), 116-120, 2022.
- [31] Orhan R, Aydođmuş E. “Investigation of some thermophysical properties of *Asphodelus aestivus* reinforced polyester composite”. *Firat University Journal of Experimental and Computational Engineering*, 1(3), 103-109, 2022.
- [32] Aydođmuş E, Dađ M. “Characterization of Thermophysical of Biomass Reinforced Polyester Composite”. *1st International Conference of Physics*, Ankara, 2021.

- [33] Ahmed F, Urooj A. “Traditional uses, medicinal properties, and phytopharmacology of *Ficus racemosa*: a review”. *Pharmaceutical Biology*, 48(6), 672-681, 2010.
- [34] Augustus GDPS, Seiler, G.J. (2011). “*Ficus elastica* – The Indian rubber tree – An underutilized promising multi-use species”. *Biomass and Bioenergy*, 35 (7), 3247-3250.
- [35] Chantarasuwan B, Tongrikem S, Pinyo P, Kanithajata P, Kjellberg F. “A natural population of *Ficus elastica* Roxb.ex Hornem. in Thailand”. *The Thailand Natural History Museum Journal*, 10, 7–14, 2016.
- [36] De-Amorin AH, Borba HR, Carauta LD, Kaplan MA. “Anthelmintic activity of the latex of *Ficus carica*”. *Journal of Ethnopharmacology*, 64, 255–258, 1999.
- [37] Galati EM, Monforte MT, Tripodo MM, D’aquino A, Mondello MR. “Antiulcer activity of *Opuntia Ficus Indica* (L.) Mill. (Cactaceae): ultrastructural study”. *Journal of Ethnopharmacology*, 76, 1–9, 2001.
- [38] Kiem PV, Minh CV, Nhiem NX, Tai BH, Quang TH, Anh HLT, Cuong NX, Hai TN, Kim SH, Kim JK, Jang HD, Kim YH. “Chemical constituents of the *Ficus elastica* leaves and their antioxidant activities”. *The Bulletin of the Korean Chemical Society*, 33(10), 3461-3464, 2012.
- [39] Aydođmuş E, Dađ M, Yalçın ZG, Arslanođlu H. “Synthesis and characterization of EPS reinforced modified castor oil-based epoxy biocomposite”. *Journal of Building Engineering*, 47, 103897, 2022.
- [40] Şahal H, Aydođmuş E. “Production and Characterization of Palm Oil Based Epoxy Biocomposite by RSM Design”. *Hittite Journal of Science and Engineering*, 8(4), 287-297, 2021.
- [41] Aydođmuş E, Şahal H. “Polyester and Epoxy Hybrid-Composite Production and Characterization”. *13th International Conference of Strategic Research on Scientific Studies and Education*, Antalya, 2021.
- [42] Aydođmuş E, Arslanođlu H. “Kinetics of thermal decomposition of the polyester nanocomposites”. *Petroleum Science and Technology*, 39(13–14), 484–500, 2021.
- [43] Aydođmuş E. “Biohybrid nanocomposite production and characterization by RSM investigation of thermal decomposition kinetics with ANN”. *Biomass Conversion and Biorefinery*, 12, 4799-4816, 2022.

Detection of brain tumor with a pre-trained deep learning model based on feature selection using MR images

MR görüntüleri kullanılarak öznelik seçimine dayalı ön-eğitilmiş bir derin öğrenme modeliyle beyin tümörünün tespiti

Kürşat DEMİR¹ , Berna ARI² , Fatih DEMİR^{3*} 

¹Department of Mechatronics Engineering, Faculty of Technology, Firat University, Elazig, Turkey.

²Department of Electrical-Electronic Technologies, Faculty of Technology, Firat University, Elazig, Turkey.

³Department of Biomedicine, Vocational School of Technical Sciences, Firat University, Elazig, Turkey.

¹kursatdemir62@gmail.com, ²bernagurler@gmail.com, ³fatihdemir@firat.edu.tr

Received: 14.01.2023
Accepted: 26.01.2023

Revision: 19.01.2023

doi: 10.5505/fujece.2023.36844
Research Article

Abstract

One of the most dangerous diseases in the world is a brain tumor. A brain tumor destroys healthy tissue in the brain and then multiplies abnormally, causing increased internal pressure in the skull. This can lead to death if not diagnosed early. Magnetic Resonance Imaging (MRI) is a diagnostic method that is frequently used in soft tissues and gives successful results. In this study, a brain tumor was automatically detected from MR images. For feature extraction, a pre-trained Convolutional Neural Network (CNN) model named MobilenetV2 was used. Then, the ReliefF algorithm was used for feature selection. The features extracted with MobileNetV2 and the features selected with the ReliefF algorithm are given separately to the classifiers and the system performance is tested. As a result of experimental studies, it was seen that the highest performance was obtained with the combination of MobileNetV2 feature extraction, ReliefF algorithm feature selection, and KNN classifier.

Keywords: Feature selection, ReliefF algorithm, MobileNetV2, brain tumor, Magnetic resonance imaging

Özet

Dünyadaki en tehlikeli hastalıklardan biri beyin tümörüdür. Bir beyin tümörü beyindeki sağlıklı dokuyu yok eder ve daha sonra anormal şekilde çoğalarak kafatasında iç basıncın artmasına neden olur. Bu erken teşhis edilmezse ölüme yol açabilir. Manyetik Rezonans Görüntüleme (MRG) yumuşak dokularda sıklıkla kullanılan ve başarılı sonuçlar veren bir tanı yöntemidir. Bu çalışmada, MR görüntülerinden bir beyin tümörü otomatik olarak tespit edildi. Öznelik çıkarımı için MobilenetV2 adlı önceden eğitilmiş bir Evrişimsel Sinir Ağı modeli kullanılmıştır. Daha sonra öznelik seçimi için ReliefF algoritması kullanılmıştır. MobileNetV2 ile çıkarılan öznelikler ve ReliefF algoritması ile seçilen öznelikler ayrı ayrı sınıflandırıcılara verilerek sistem performansı test edilmiştir. Deneysel çalışmalar sonucu MobileNetV2 öznelik çıkarımı, ReliefF algoritması öznelik seçimi ve KNN sınıflandırıcı kombinasyonu en yüksek başarımın elde edildiği görülmüştür.

Anahtar kelimeler: Öznelik seçimi, ReliefF algoritması, MobileNetV2, Beyin tümörü, Manyetik rezonans görüntüleri

1. Introduction

The brain is one of the body's most intricate organs. A brain tumor is a clump of tissue that develops and multiplies uncontrolled in the brain [1]. The American Society of Clinical Oncology estimates that between 85.0% and 90% of the brain, cancers are malignancies of the central nervous system [2]. Despite being less frequent than other tumor forms in the central nervous system, brain tumors in particular have a high death rate. Therefore, the efficacy of treatment and the reduction of mortality from brain tumors depend greatly on early identification [3].

MRI is superior to other imaging methods like computed tomography (CT) and positron emission tomography in several ways (PET). Magnetic resonance imaging (MRI) technologies offer researchers more detailed, increased contrast images of the brain for the detection of brain malignancies. Additionally, MRI is a non-invasive method that is safe for the human

*Corresponding author

body. Additionally, MRI technology is quick and takes less time to finish treatments. Consequently, MRI has emerged as the method of choice in clinical practice for finding brain tumors [4].

The use of clinical information and qualified radiologists and other specialists is essential for the early diagnosis of brain tumors. Decision-making processes for the detection of brain tumors might be time-consuming due to the shortage of professionals in healthcare. Computer-aided systems powered by artificial intelligence can lessen professionals' workloads and help them make decisions [4,5].

Traditional approaches could work well for one dataset but poorly for another since the right features must be extracted for each data format. Convolution filters found in deep learning architectures eliminate the requirement for manual feature extraction. Because of this, deep learning-based studies have excelled at several tasks involving the classification of medical images [6–20]. A pre-trained CNN-based model was utilized by Lu et al. [21] to identify brain cancers in MRI images. The MobileNetV2 model's deep features were extracted. The random vector functional-network approach had a classification accuracy of 96.0%. The binary classification had a classification accuracy of over 95.0%. For brain MRI classification, Taló et al. [22] used five pre-trained CNN networks, including AlexNet, VGG16, ResNet (18, 34, and 50) models. ResNet50 had the best accuracy, 95.23%. A unique strategy for brain MRI categorization including various processes was reported by Kumar and Mankame [23]. For segmentation, a combination fuzzy structure and a sine-cosine algorithm were employed. The segmented images were then utilized to extract features using a statistical method and a local binary model (LBP). In order to categorize data, a deep CNN model that was built from scratch was used. The method's highest degree of accuracy was 96.23%.

To identify the two types of brain tumors that fall under the deep autoencoder model, low- and high-grade gliomas, Raja and Siva [24] developed an architecture. First, a median filter was used to preprocess MR images. Second, segmentation was accomplished using a Bayesian clustering approach. An end-to-end learning deep autoencoder model was used to classify the MR image samples. The approach had a 98.5% accuracy rate. A unique CNN model was chosen by Devi and Gomathi [25] for automatic brain tumor identification. For preprocessing, a canny edge detection technique was applied. Then, MR sample saliency map representations were created. A CNN model with five convolutional layers was used for the prediction procedure, yielding 91.0% accuracy. For the 3-class (glioma, meningioma, and pituitary tumor) brain MRI classification, Alhassan and Zainon [26] suggested a deep CNN structure based on a hard swish-based ReLU activation function. The classification performance was enhanced by 3.5% accuracy thanks to the hard swish-based ReLU activation function, with the highest accuracy being 98.26%. For the classification of brain tumors, Kumar et al. [27] used a ResNet50-based method that included the glioma, meningioma, and pituitary classifications. The accuracy results were 97.48% and 97.08%, respectively, with and without data augmentation. A unique method for classifying brain tumors into three categories was devised by Kokkala et al. [128]. To identify glioma, meningioma, and pituitary samples, a deep dense initial residual network was trained. The model had a 99.26% average accuracy. A unique strategy for 2-class brain MR image categorization was put forth by Mesut et al. [29]. In this method, deep feature extraction was carried out using two pre-trained CNN models, VGG16 and AlexNet. Moreover, all CNN models' convolutional layers were subjected to the Hypercolumn method. As a result, the deep feature set now includes local discriminative features. Out of the 2000 features collected, 200 features with good representativeness were chosen using the recursive feature elimination (RFE) algorithm. The SVM classifier's greatest accuracy was 96.77%. A strategy based on deep feature extraction was put out by Kang et al. [30] for the classification of 4-class brain MRI images. Popular pre-trained CNN models like ResNet, DenseNet-169, VGGNet, AlexNet, Inceptionv3, ResNeXt, ShuffleNet, MobileNetV2, and MnasNet were used to extract deep features. In order to achieve the best feature performance, DenseNet-169, ShuffleNet, and MnasNet models were combined. Several classifier techniques, including Adaboost, Gaussian Naive Bayes, K-Nearest Neighbor (KNN), Random Forest, and Support Vector Machine (SVM), were utilized in the classification phase. The SVM classifier produced the best classification results. 93.72% accuracy was the highest. A novel method for tumor detection and tumor classification from brain MR images was developed by Arı et al. [31]. First, a Gaussian filter is used to preprocess MR images of the brain. Then, using the proper threshold and morphological operations, malignancies were found. Different combinations of deep features were recovered from the fc6 and fc7 layers of the AlexNet and VGG16 models. In the classification phase, ELM was utilized. On three datasets, the proposed method's effectiveness was evaluated.

2. Preliminaries

Classifiers

The Linear discriminant (LD) method is frequently used in both classification and feature reduction. LD assumes that each class produces different Gaussian distributions. LD then finds the best decomposition by considering the maximum variance between classes [32]. SVM is a commonly used supervised machine learning method. The main idea behind SVM is Vapnik's statistical learning theory. SVM projects the input data into higher dimensional space and builds the hyperplane to separate classes in the projected space. Basically, SVM solves linear problems. For solving nonlinear problems, SVM uses nonlinear kernel functions such as Gaussian, sigmoid, and polynomial [33]. KNN is a fundamental and widely used supervised machine learning technique. KNN uses local knowledge of the predicted input data, so it is a feasible and adaptive method. KNN solves the problem by considering the input data point neighbor relations. KNN uses distance metrics such as Euclidean, Minkowski, Manhattan, Manhattan, Cosine, Hamming, etc. to detect the neighborhood relationship. The k closest instances are selected from the input data, then any class is assigned according to the majority relations. The number of neighbors, k , should be an odd number to avoid ambiguity [34]. Decision Trees (DT) are a tree-based algorithm used in classification and regression problems and are one of the most widely used predictive methods. Each node in the tree represents a test on a feature. Node branches indicate the result of the test. Tree leaves contain the class labels. Decision tree inference consists of tree construction and tree cleaning phases [35].

MobileNetV2

Sandler [36] has suggested MobileNetV2, a CNN architecture for mobile devices. The initial version, which was created for face feature detection, was tested and trained using data from Google [37]. An inverted residual and a linear bottleneck are used in the network structure that was created. It is intended for generic feature extraction as well as image categorization. This network implements bottleneck operations, mean pooling, 3×3 and 1×1 convolution. Layers in MobileNetV2 total 154. Compared to other popular CNN models, MobileNetV2 employs fewer parameters [38]. An effective network design with rapid execution is MobileNetV2. Figure 1 displays the MobileNetV2 convolutional blocks.

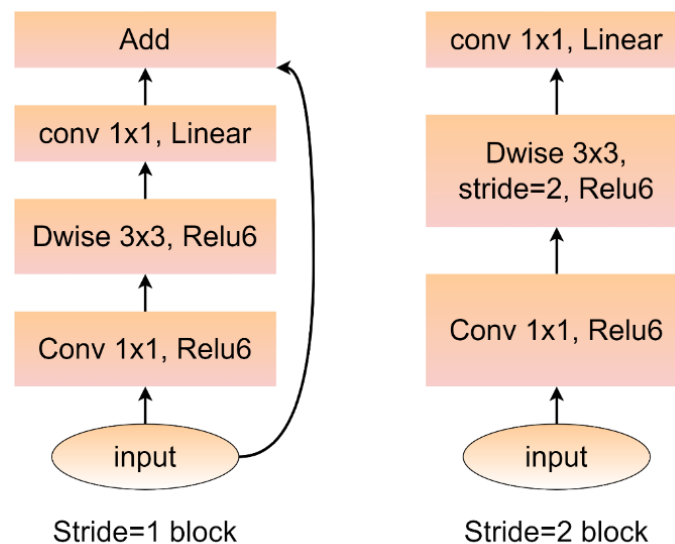


Figure 1. MobileNetV2 convolutional blocks

Relief family of algorithm

Kira and Rendell developed the Relief algorithm in 1992, which is highly sensitive to feature interactions and uses a filter-method approach to feature selection [39]. It was initially intended for use in discrete or numerical feature binary classification issues. Each feature in Relief has a feature score, which may be used to rank and select the features with the

highest scores. Further modeling can be guided by these scores, which can also serve as feature weights. Relief feature scoring is built on the identification of feature value differences between nearest neighbor instance pairs. If a close instance pair of the same class exhibits a variation in feature value, the feature score is reduced (a "hit"). As an alternative, the feature score increases if a neighboring instance pair with a different class value exhibits a feature value difference (a "miss") [40].

3. Method

The framework of the proposed approach is given in Figure 2. In this study, a novel approach for automatic ophthalmologic disease detection from MR images is proposed. In the first step, deep features are extracted from the pre-trained MobileNetV2 ESA model. In the second step, discriminative features are selected using a multi-level algorithm with INCA algorithms[41-43]. This algorithm improves the classification performance and reduces the computational cost of the classifier. At the third level, the selected features are passed to the SVM classifier.

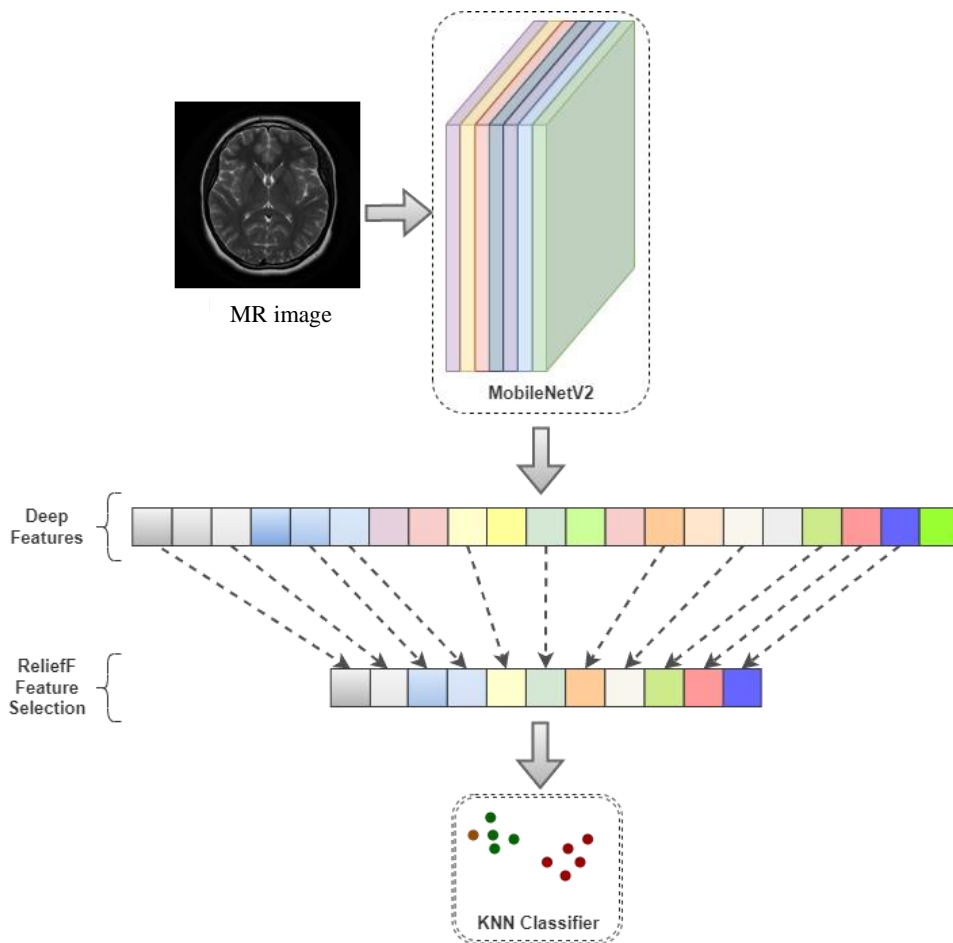


Figure 2. Proposed approach architecture

4. Experiments and discussion

On a dataset that is available to the public, the suggested approach was assessed. The collection included MR pictures of both brain tumors and healthy individuals [44]. 155 cases of brain tumors and 98 cases of healthy tissue resulted in the collection of 253 MR images. The MR pictures were stored in JPEG format with various resolutions and size settings. The dataset examples are provided in Figure 3.

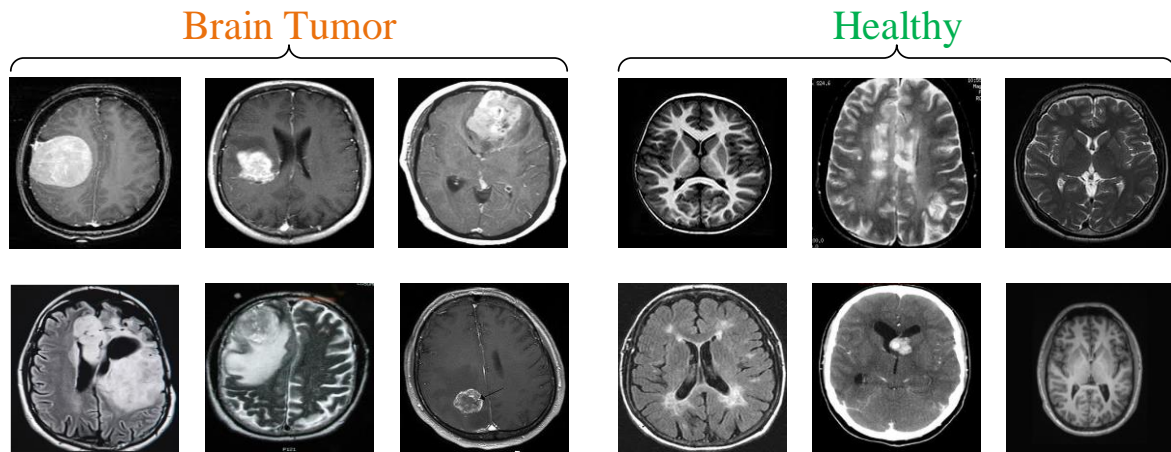


Figure 3. Samples for each class on the datasets

The study's entire coding was carried out using Matlab software. The PC used in the study has 16 GB of main memory, an Intel i5 processor, and a 4 GB video card. A fully connected layer of the MobileNetV2 ESA model called "Logits" was utilized for the extraction of deep features, and 1000 deep features were recovered from it. After that, the ReliefF feature selection technique was applied to boost classification performance while lowering computing costs. The number of nearest neighbors, a crucial parameter in this technique, was set at 10. Figure 4 provides a representation of the feature weights computed using this technique.

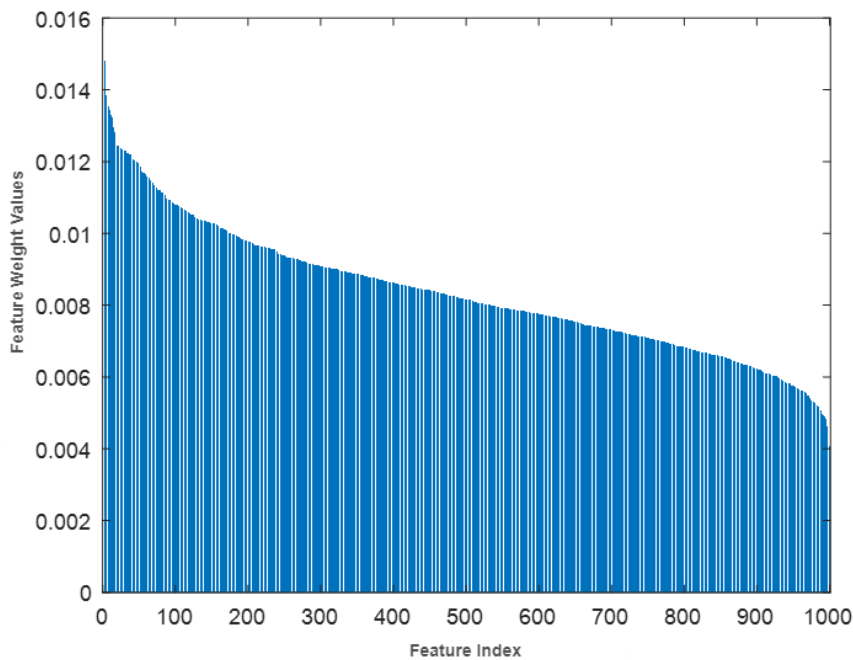


Figure 4. Feature weights calculated with the ReliefF algorithm

The weight values of these computed attributes were used to choose the first 300 attributes. The Matlab Classification Learner tool received these features for classification. The evaluation method was 10-fold cross-validation. This procedure was repeated twice, once before feature selection and once after. Table 1 provides the categorization accuracy results from this technique.

Table 1. Classification performance

Classifier	All features	Selected features (with ReliefF)
DT	0.88	0.91
LD	0.86	0.90
SVM	0.92	0.94
KNN	0.95	0.99

As shown in Table 1, the ReliefF feature selection algorithm improved the performance of all classifiers. The best classification performance was obtained with the KNN algorithm (0.99).

The complexity matrices in Figure 5 are given to see the effect of feature selection on classification performance. As demonstrated above, the ReliefF algorithm increased the number of predicted instances in both classes and as a result, the accuracy was improved by 4%.

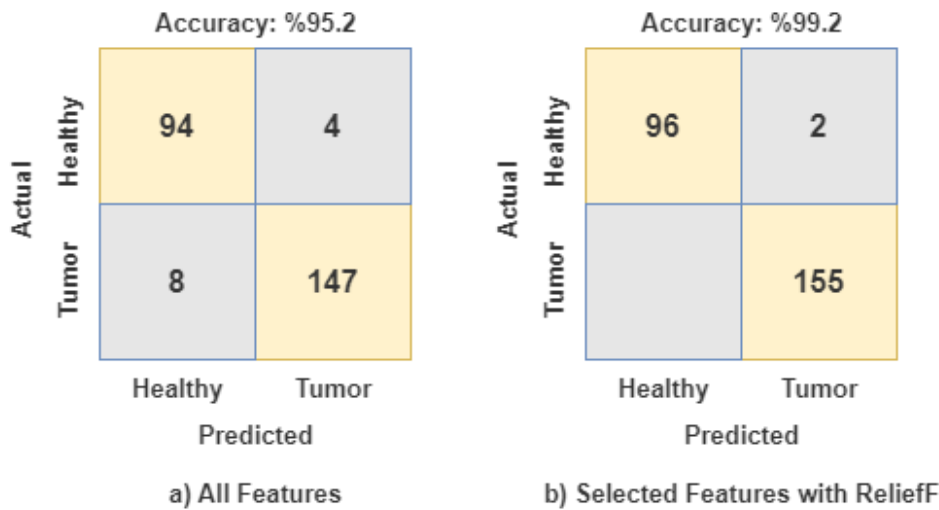


Figure 5. ReliefF impact of feature selection on performance

When the studies conducted with the same data are examined, Table 2 presents the general summary. Nanda et al. [45] emphasized that they used a new hybrid saliency k-mean segmentation (Saliency-K-mean-SSO-RBNN) by taking advantage of the social spider optimization (SSO) algorithm in their study in the Radial Basis Neural Network (RBNN). The saliency map focuses on the relevant point in the target image. It was reported that 96%, 92%, and 94% accuracy were obtained in the study, in which processes were tested with three different data sets. Demir and Akbulut [46], used the convolution and fully connected layers of a new R-CNN model in the deep feature extraction phase. Among the features obtained, the 100 most dominant features in terms of distinctiveness were selected with the LINSR algorithm. The best performance in the classification phase was obtained with SVM using the Gaussian kernel. In addition, in the study, the method was tested with another data set with four classes and 96.6% accuracy was achieved. Alnabhan et al. [47] wanted to reduce the complex relationship of CNN parameters by using Egyptian Vulture Optimization (EVO) technique in their study. They also tested their methods, which they tested with ANN and deep learning-based classifiers, on another data set with four classes. Asif et al. [48], tested their proposed method with two different data sets in their study. Preprocessed MR images were exported to Xception, NasNet Large, DenseNet121, and InceptionResNetV2. They used ADAM, SGD, and RMSprop algorithms as optimizers when using MR images for testing. They obtained 99.67% accuracy by using the Xception model with the data set having a larger sample size.

Table 2. Comparison of current studies with the same data set [43]

Reference	Method	Classification	(Acc.%)
Nanda et al. (2023)	Saliency-K-mean-SSO	RBNN	%92
Demir and Akbulut (2022)	R-CNN, L1NSR	SVM	%98.8
Alnabhan et al. (2022)	CNN-based EVO model	CNN	%93.51
Asif et al. (2022)	Xception, ADAM optimization	Xception	%91.94
Proposed Method	MobileNetV2, ReliefF algorithm	KNN	%99

5. Conclusion

In this study, a deep learning-based hybrid technique for the classification of brain tumors is presented. In the study, deep features were extracted with the pre-trained MobileNetV2 architecture. It is desired to reduce the computational cost and processing load without transmitting the features to the KNN algorithm, which is a powerful classifier. The ReliefF algorithm is used for the mentioned feature extraction step. In order to see the performance effect of the algorithm on the designed model, the model in which all the features are added to the system and the situation after the feature selection is given to the classifier separately. As a result of the comparison, it was concluded that the classification performed 2% better, and ultimately a high accuracy of 99% was achieved. The mentioned success rate can be a helpful system for experts since the treatment and diagnosis stage of brain tumors is considered to be of critical importance. In future studies, it is planned to test CNN models trained from scratch on the same dataset to improve classification accuracy.

6. Acknowledgements

We would like to thank the researcher for providing a publicly available dataset [44].

7. Author Contribution Statement

All the authors in this research made one or two contributions toward the success of this research. Author 1, provided the finite element solution of the diffusivity equation while Author 2 used the result from the first author to analyze the reservoir production rate and cumulative production. Authors 2 and 3 supervised the research and help in the validation of the result using relevant literature.

8. Ethics Committee Approval and Conflict of Interest

There is no need for an ethics committee approval in the prepared article and there is no conflict of interest with any person/institution in the prepared article.

9. References

- [1] Havaei M, Davy A, Warde-Farley D, Biard A, Courville A, Bengio Y, Pal C, Jodoin PM, Larochelle H. "Brain tumor segmentation with Deep Neural Networks". *Medical Image Analysis.*, 35, 18–31, 2017.
- [2] American Society of Clinical Oncology. <https://www.cancer.net/cancer-types/brain-tumor/statistics>
- [3] Petruzzi A, Finocchiaro CY, Lamperti E, Salmaggi A. "Living with a brain tumor", *Supportive. Care in Cancer.* 21(4), 1105–1111, 2013.
- [4] Mohammed M, Nalluru SS, Tadi S, Samineni R. "Brain tumor image classification using convolutional neural networks". *Int. J. Adv. Sci. Technol.* 29(5), 928–934, 2019.

- [5] Ucuz I, Ari A, Ozcan OO, Topaktas O, Sarraf M, Dogan O. “Estimation of the development of depression and PTSD in children exposed to sexual abuse and development of decision support systems by using artificial intelligence”. *Journal of child sexual abuse*, 31(1), 73-85, 2022.
- [6] Tasci I, Tasci B, Doğan S, Tuncer T. “A new dataset for EEG abnormality detection MTOUH”. *Turkish Journal of Science and Technology*, 17(1), 135-141, 2022.
- [7] Toğaçar M, Cömert Z, Ergen B. “Intelligent skin cancer detection applying autoencoder, MobileNetV2 and spiking neural networks”. *Chaos, Solitons and Fractals*, 144, 110714, 2021.
- [8] Demir F, Tasci B. “An Effective and Robust Approach Based on R-CNN+ LSTM Model and NCAR Feature Selection for Ophthalmological Disease Detection from Fundus Images”. *Journal of Personalized Medicine*, 11(12), 1276, 2021.
- [9] Tasci B. “Ön Eğitilmiş Evrişimsel Sinir Ağları Modellerinde Öznelik Seçim Algoritmasını Kullanarak Cilt Lezyon Görüntülerinin Sınıflandırılması”. *Firat Üniversitesi Mühendislik Bilimleri Dergisi*, 34(2), 541-552, 2022.
- [10] Loh HW, Ooi CP, Aydemir E, Tuncer T, Dogan S, Acharya UR. “Decision support system for major depression detection using spectrogram and convolution neural network with EEG signals” *Expert Systems*, 39(3), e12773, 2022.
- [11] Tasci B, Tasci G, Dogan S, Tuncer T. “A novel ternary pattern-based automatic psychiatric disorders classification using ECG signals”. *Cognitive Neurodynamics*, 1-14, 2022.
- [12] Demir F, Akbulut Y, Taşcı B, Demir K. “Improving brain tumor classification performance with an effective approach based on new deep learning model named 3ACL from 3D MRI data”. *Biomedical Signal Processing and Control*, 81, 104424, 2023.
- [13] Tasci G, Loh W, Barua D, Baygin M, Tasci B, Dogan S, Acharya, UR. “Automated accurate detection of depression using twin Pascal’s triangles lattice pattern with EEG Signals”. *Knowledge-Based Systems*, 260, 110190, 2023.
- [14] Dogan S, Baygin M, Tasci B, Loh HW, Barua PD, Tuncer T, Acharya UR. “Primate brain pattern-based automated Alzheimer’s disease detection model using EEG signals”. *Cognitive Neurodynamics*, 1-13, 2022.
- [15] Tasci B. “Beyin MR görüntülerinden mrmr tabanlı beyin tümörlerinin sınıflandırılması”. *Journal of Scientific Reports-B*, 6, 1-9, 2022.
- [16] Tasci B. “A Classification Method for Brain MRI via AlexNet”. *International Conference on Disruptive Technologies for Multi-Disciplinary Research and Applications (CENTCON)*, IEEE, 347-35, 2021.
- [17] Karadal CH, Kaya MC, Tuncer T, Dogan S, Acharya UR. “Automated classification of remote sensing images using multileveled MobileNetV2 and DWT techniques.”, *Expert Systems with Applications*, 185, 115659, 2021.
- [18] Demir F. “DeepCoroNet: A deep LSTM approach for automated detection of COVID-19 cases from chest X-ray images”, *Applied Soft Computing*, 103, 107160, 2021.
- [19] Demir F. “DeepBreastNet: A novel and robust approach for automated breast cancer detection from histopathological images”. *Biocybernetics and Biomedical Engineering*, 41(3), 1123–1139, 2021.
- [20] Talo M, Yildirim O, Baloglu UB, Aydin G, Acharya UR. “Convolutional neural networks for multi-class brain disease detection using MRI images”. *Computerized Medical Imaging and Graphics*, 78, 101673 2019.
- [21] Lu SY, Wang SH, Zhang YD. “A classification method for brain MRI via MobileNet and feedforward network with random weights”. *Pattern Recognit. Lett.* 140, 252–260, 2020.
- [22] Talo M, Baloglu UB, Yildirim Ö, Acharya UR. “Application of deep transfer learning for automated brain abnormality classification using MR images”. *Cognitive Systems Research*, 54, 176–188, 2019.
- [23] Kumar S, Mankame DP. “Optimization driven Deep Convolution Neural Network for brain tumor classification”. *Biocybern. Biomed. Eng.*, 40(3), 1190–1204, 2020.
- [24] Raja PMS. “Brain tumor classification using a hybrid deep autoencoder with Bayesian fuzzy clustering-based segmentation approach”. *Biocybern. Biomed. Eng.*, 40(1), 440–453, 2020.
- [25] Devi UK, Gomathi R. “Brain tumour classification using saliency driven nonlinear diffusion and deep learning with convolutional neural networks (CNN)”. *Journal of Ambient Intelligence Humanized Computing*, 12(6), 6263–6273, 2021.
- [26] Alhassan AM, Zainon WMNW. “Brain tumor classification in magnetic resonance image using hard swish-based RELU activation function-convolutional neural network”. *Neural Computing and Applications*, 33(15), 9075–9087, 2021.
- [27] Kumar RL, Kakarla J, Isunuri BV, Singh M. “Multi-class brain tumor classification using residual network and global average pooling”. *Multimedia Tools and Applications*, 80(19), 13429–13438, 2021.
- [28] Kokkalla S, Kakarla J, Venkateswarlu IB, Singh M. “Three-class brain tumor classification using deep dense inception residual network”. *Soft Computing*, 25(13), 8721–8729, 2021.
- [29] Toğaçar M, Cömert Z, Ergen B. “Classification of brain MRI using hyper column technique with convolutional neural network and feature selection method”. *Expert Systems with Applications*, 149, 113274, 2020.
- [30] Kang J, Ullah J, Gwak J. “Mri-based brain tumor classification using ensemble of deep features and machine learning classifiers”. *Sensors*, 21(6) 1–21, 2021.
- [31] Arı A, Alcin OF, Hanbay D. “Brain MR Image Classification Based on Deep Features by Using Extreme Learning Machines”. *Biomedical Journal of Scientific and Technical Research*, 25(3), 2020.
- [32] Alcin ÖF, Korkmaz D, Ekici S, Şengür A. “An Artificial Neural Network Model for The Amperes Law”. *Global Journal on Technology*, 4(2), 2013.

- [33] Turkoglu M, Aslan M, Ari A, Alçin ZM, Hanbay D. “A multi-division convolutional neural network-based plant identification system”. *PeerJ Computer Science*, 7, e572, 2021.
- [34] Ari A. “Analysis of EEG signal for seizure detection based on WPT”. *Electronics Letters*, 56(25), 1381-1383, 2020.
- [35] Ari B, Ucuz I, Ari A, Ozdemir F, Sengur A. “Grafik Tablet Kullanılarak Makine Öğrenmesi Yardımı ile El Yazısından Cinsiyet Tespiti”. *Firat Üniversitesi Mühendislik Bilimleri Dergisi*, 32(1), 243-252, 2020.
- [36] Sandler M, Howard A, Zhu M, Zhmoginov A, Chen LC, “MobileNetV2: Inverted Residuals and Linear Bottlenecks,” *Proceedings of the IEEE conference on computer vision and pattern recognition*, 4510-4520, Jan 2018.
- [37] Howard AG, Zhu M, Chen B, Kalenichenko D, Wang W, Weyand T, Andreetto M, Adam H, “MobileNets: Efficient Convolutional Neural Networks for Mobile Vision Applications”. *arXiv*, 1704.04861, 2017.
- [38] Karadal CH, Kaya M, Tuncer T, Dogan, S, Acharya UR. “Automated classification of remote sensing images using multileveled MobileNetV2 and DWT techniques”. *Expert Systems with Applications*, 185, 115659, 2021.
- [39] Kira, K, Rendell LA. “The feature selection problem: Traditional methods and new algorithm”. *Proceedings of AAAI’92*, 2, 129-134, 1992.
- [40] Kira K, Rendell LA. “A practical approach to feature selection”. *Machine Learning: Proceedings of International Conference (ICML’92)*, 249–256, 1992.
- [41] Tasci B, Tasci I. “Deep feature extraction based brain image classification model using preprocessed images: PDRNet”. *Biomedical Signal Processing and Control*, 78, 103948, 2022.
- [42] Macin G, Tasci B, Tasci I, Faust O, Barua PD, Dogan S, Acharya UR. “An Accurate Multiple Sclerosis Detection Model Based on Exemplar Multiple Parameters Local Phase Quantization: ExMPLPQ”. *Applied Sciences*, 12(10), 4920, 2022
- [43] Demir K, Ay M, Cavas M, Demir F. “Automated steel surface defect detection and classification using a new deep learning-based approach”. *Neural Computing and Applications*, 1-18, 2022.
- [44] Chakrabarty N. “Brain MRI images for brain tumor detection”. <https://www.kaggle.com/navoneel/brain-mri-images-for-brain-tumor-detection/metadata>
- [45] Nanda A, Barik RC, Bakshi S. “SSO-RBNN driven brain tumor classification with Saliency-K-means segmentation technique”. *Biomedical Signal Processing and Control*, 81, 104356, 2023.
- [46] Demir F, Akbulut Y. “A new deep technique using R-CNN model and L1NSR feature selection for brain MRI classification. *Biomedical Signal Processing and Control*”. 75, 103625, 2022.
- [47] Alnabhan M, Habboush AK, Abu QA, Mohanty AK, Pattnaik S, Pattanayak BK. “Hyper-Tuned CNN Using EVO Technique for Efficient Biomedical Image Classification”. *Mobile Information Systems*, 2022, 2022.
- [48] Asif S, Yi W, Ain QU, Hou J, Yi T, Si J. “Improving Effectiveness of Different Deep Transfer Learning-Based Models for Detecting Brain Tumors From MR Images”. *IEEE Access*, 10, 34716-34730, 2022.



An examination of synthetic images produced with DCGAN according to the size of data and epoch

DCGAN ile üretilen sentetik görüntülerin veri boyutuna ve epoch sayısına göre incelenmesi

Canan KOÇ^{1*} , Fatih ÖZYURT² 

^{1,2} Department of Software Engineering, Faculty of Engineering, Firat University, Elazig, Turkey.

¹canan.koc@firat.edu.tr, ²fatihozyurt@firat.edu.tr

Received: 13.09.2022

Accepted: 17.10.2022

Revision: 07.10.2022

doi: 10.5505/fujece.2023.69885

Research Article

Abstract

In recent years, the popular network of adversarial networks has increased in studies for computer vision. The lack of data used in the studies and the lack of good training for the resulting model draw attention to techniques such as data enhancement and synthetic data generation. In this article, synthetic data was produced using Generative Adversarial Networks (GANs). The data in the dataset used consists of 10000 faces from the CelebA dataset available online. The impact of the increase in the number of data on fake images created by DCGAN, one of the GANs, is the main topic of the article. In the study, the data is divided into two parts. In the first study, fake data were generated from 5000 data, and in the next study, fake data images were forged using all of the data meaning 10000 data. The result was found that the number of data and the increase in epoch were accurately proportional to the success of the fraudulent images created.

Keywords: Generative adversarial networks, Synthetic data, Generative model

Özet

Son yıllarda Bilgisayarla Görü için yapılan çalışmalarda Çekişmeli Ağlar'ın popülerliği artmıştır. Yapılan çalışmalarda kullanılan verilerin yetersiz oluşu ve bunun sonucunda oluşturulan modelin iyi eğitilememesi veri artırma ve sentetik veri üretme gibi tekniklere dikkat çekmektedir. Bu makalede yapılan çalışmada Çekişmeli Üretici Ağlar (GANs) kullanılarak sentetik veri üretimi yapılmıştır. Kullanılan veri setindeki veriler çevrimiçi olarak bulunan CelebA veri setinden alınan 10000 yüz görüntüsünden oluşmaktadır. Veri sayısındaki artışın GANs çeşitlerinden biri olan DCGAN tarafından oluşturulan sahte görüntüler üzerindeki etkisi makalenin ana konusudur. Yapılan çalışmada veriler ikiye ayrılarak kullanılmıştır. İlk yapılan çalışmada 5000 veri, sonraki çalışmada ise 10000 verinin tamamı kullanılarak sahte yüz görüntüleri oluşturulmuştur. Alınan sonuçta ise veri sayısının ve epoch sayısının artışının oluşturulan sahte görüntülerin başarısıyla doğru orantılı olduğu görülmüştür.

Anahtar kelimeler: Çekişmeli üretici ağlar, Sentetik veri, Üretici model

1. Introduction

Machine learning has been one of the key areas that we have recently faced in solving problems. Most of the work done in this field requires a large data size and with a large number of data, it is accurate to learn the model created in machine learning. However, there has also been an increase in the direction of this area, especially due to the lack of data sets and the difficulties in obtaining ethical board permits for the data used in the field of health. Researchers have started to look for a variety of solutions. Offering multiple solutions to these issues. Data Augmentation, GAN, and similar algorithms are examples of what can be given to these methods.

Generative Adversarial Networks, GANs, are one of the best and most useful topics in the production of fake data, first proposed by Ian Goodfellow in recent years [1-2]. Although there are many computer programs used to generate data, GANs stand out from the rest with their results and versatility. The GANs are used in many different areas, with

¹Corresponding author

many different types. StackGANs [3], CycleGANs [4], Age-cGANs [5], DCGANs [6], InfoGAN [7], Laplacian GAN [8] is just a few of them. To increase the number of data, as well as increase the resolution of the low-resolution image, Ledig and his friends recommended the SR-GANs model [9]. In addition, Xiaodong and his friends recommended the DualG-GAN model in 2022 for synthesizing from text to image [10].

In this article, DCGANs were used to produce successful face images. This DCGAN model used is the most common type of GANs model. This type of GAN is to look at the effect of the data increase on the quality of images produced by GAN.

2. Materials and Methods

2.1. Dataset

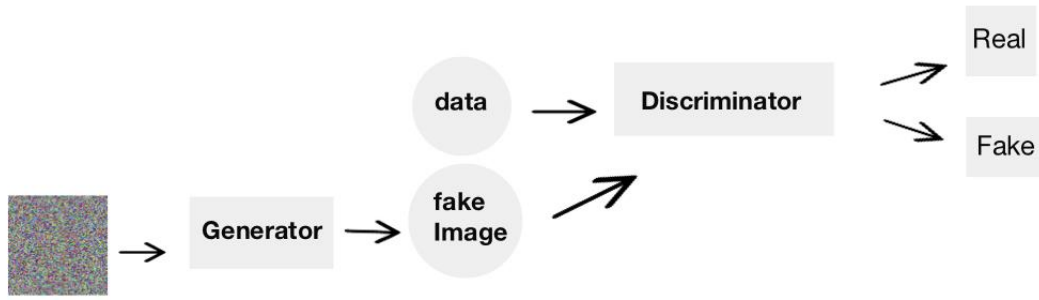
The dataset used in the study consists of 10,000 faces acquired from the dataset, CelebA, shared online [11]. Facial images are mixed as men and women in the dataset. Examples of facial images with glasses, hats, curls, straight hair, different facial shapes, and facial expressions are shown in figure 1.



Figure 1. Examples of actual face images in the dataset

Deep Convolutional Generative Adversarial Networks (DCGANs)

GANs are a machine learning technique consisting of two neural networks that are simultaneously trained [12]. The first of these networks is the Generator network, which produces the fake data, and the other is the Discriminator network, which is used to distinguish the generated fake image from the real image [13]. In general, if you look at words one at a time, the word Generative represents the purpose of the model, to produce new data. The word Adversarial represents a game between two neural networks. When the generator tries to produce the best fake image, the Discriminator tries to distinguish the generated fake image from the actual images. This struggle between the two neural networks is summarized as a game. The word Networks represents two neural networks, called the Generator and Discriminator networks at the base of the model.



Şekil 2. Generative Adversarial Networks (GANs) architecture

The GAN architecture is briefly represented as shown in figure 2. The generator receives the noise vector z first as the network input and tries to produce an image. The generated $G(z)$ dummy image is supplied as an input to the Discriminator network with the X_d actual image. In this section, the role of the Discriminator network is to perform a binary classification to distinguish the actual image (X_d) from the fake image produced by the Generator network ($G(z)$). The data are given as input, Generator mesh returns a numerical value close to 1 and accepts it as a real image. The generator considers the data from the network as a fake image and returns a numeric value close to 0.

Proposed Method

The DCGAN model used in the article consists of two boundary networks that conflict with each other, as with other GAN models. The generator network uses the Transposed convolution layer when trying to produce the fake image. The Transposed convolution layer mentioned is the exact opposite of the standard convolution process, but the process on the modified input map is the same. In addition, the Batch norm is used in the Generator network. In this process, which is called Batch Normalization, simultaneous learning is done because layers on the network do not have to wait for the previous layer to learn. This allows acceleration in the training. In general, ReLu and Tanh are used as the activation function. ReLu, one of the activation functions used, functions in intermediate layers, while Tanh functions in the last layer.

On the other hand, the second neural network, the Discriminator AG, tries to distinguish between the fake image produced by the Generator network and the actual image. This network has a standard convolution layer, known as the exact opposite of the Generator network. The activation function in the intermediate layer is LeakyReLU, and the function that functions in the last layer is the Sigmoid function. The real image of the fake image produced in the GANs is compared to the Loss function. The Loss function can be defined as what is being tried to optimize or minimize. It is a mathematical function that takes the root of the square of the difference between the actual value of an example and the prediction made and gives the error rate.

$$\text{loss} = \text{maximize} \log (D(x)) + \log(1 - D(G(z))) \quad (1)$$

$D(x)$ = Discriminator output of input

$D(G(x))$ = Discriminator output of fake image

In the training part of the model, the best result is to create fake images by selecting 30 epochs. To summarize the operations carried out in the study:

$$\text{Min max } V(D, G) = [E_{x \sim p_{\text{data}}(x)} [\log D(x)]] + [E_{z \sim p_z(z)} [\log (1 - D(G(z)))] \quad (2)$$

Part (1) of the equation tries to maximize output, while part (2) tries to minimize output. x is the actual image sample, and z is the noise given to the generating network to generate the image. The probability of a real picture being real is 1. The probability of a fake picture being real is 0. The values of the discriminant network are at each iteration during the training; It is updated to change the value it gives to the real image to 1 and the value it gives to the fake image to 0. The producer network is trained to ensure that the fake images it produces are close to the truth, that is,

it is evaluated as 1. The Generating Network also wants to reduce this error to 0 at each iteration. In this way, as the training process progresses, the discriminating network becomes more successful in distinguishing between real and fake images. The generative network produces more realistic fake images.

3. Experimental Results

Fake face images were created using DCGAN from face images from the CelebA dataset performed in the study. The operation consists of two parts. In the first part, 5000 faces, half of our data set, were used. When the data was trained during operation, work was carried out using different epoch numbers. The increase in Epoch has positively impacted the success of false images (fig. 3, 4, 5, and 6).



Figure 3. Fake face images produced with 5,000 data (10epoch)



Figure 4. Fake face images produced with 5,000 data (20epoch)

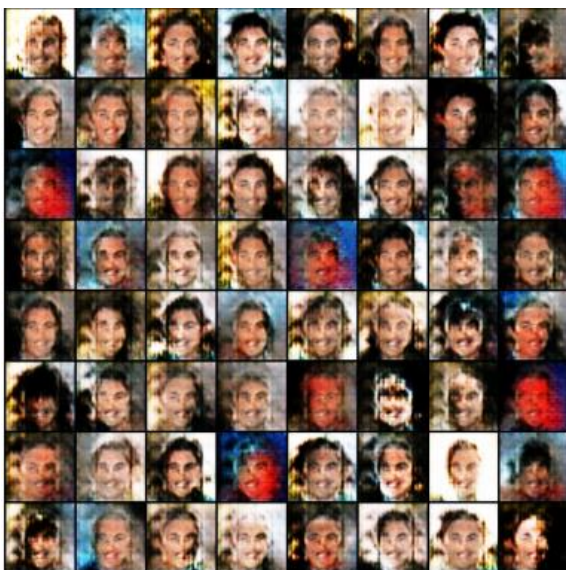


Figure 5. Fake face images produced with 5,000 data (30epoch)



Figure 6. Fake face images produced with 5,000 data (40epoch)

In the second part of the study, all the data contained in the dataset, all 10000 data, are included in the study. Fake images produced have become clearer with an increase in the number of data. This section has also tried different epoch numbers, and the best result is when 40 epoch is selected (fig. 7, 8, 9, and 10).

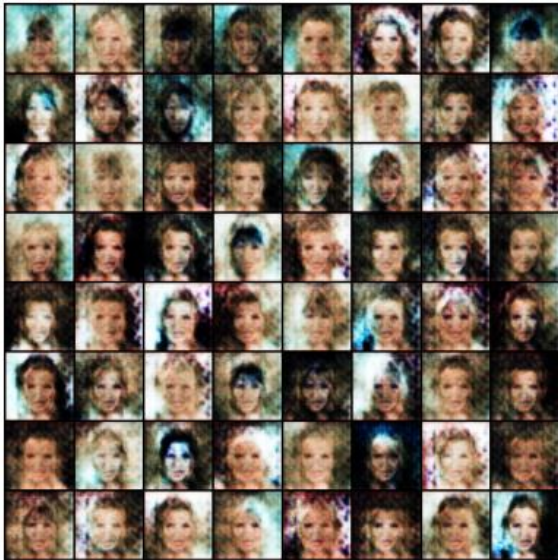


Figure 7. Fake face images produced with 10000 data (10epoch)



Figure 8. Fake face images produced with 10000 data (20epoch)

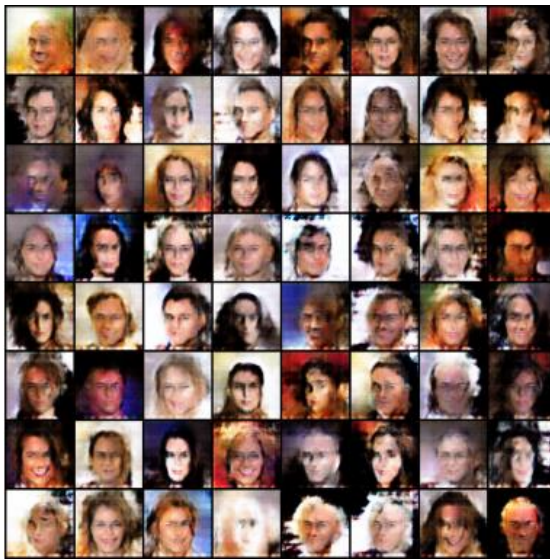


Figure 9. Fake face images produced with 10000 data (30epoch)



Figure 10. Fake face images produced with 10000 data (40epoch)

4. Conclusion

As a result of the study, it was seen that the amount of increase in the number of data caused a significant change in the clarity of the fake images. Likewise, the effect of the increase in the number of epochs on the result of the study is noticeable. In future studies, significant changes can be made in the clarity of the fake images to be produced with GAN, with a higher number of data and the addition of changes in the number of epochs. This study can be the basis of many studies.

5. Author Contribution Statement

In this study, Author 1 contributed to making the design, and literature review, contributed to forming the idea, and the analysis of results; Author 2 contributed to checking the spelling and checking in terms of content.

6. Ethics Committee Approval and Conflict of Interest

There is no need for an ethics committee approval in the prepared article. There is no conflict of interest with any person/institution in the prepared article.

7. References

- [1] Sim E-A, Lee S, Oh J, Lee J. “Gans and dcgans for generation of topology optimization validation curve through clustering analysis”. *Advances in Engineering Software*, 152, 102957, 2021.
- [2] Goodfellow I, Pouget-Abadie J, Mirza J, Xu M, Warde-Farley B, Ozai D, Courville S, Bengio, Y. “Generative adversarial networks”. *Curran Associates, Inc.*, 27, 2014.
- [3] Zhang H, Xu T, Li H, Zhang S, Wang, X, Huang X, Metaxas D. “Stackgan: Text to photo-realistic image synthesis with stacked generative adversarial networks”. *Institute of Electrical and Electronics Engineers Inc.*, 5908-5916, 2017.
- [4] Zhu J.-Y, Park T, Isola P, Efros AA. “Unpaired image-to-image translation using cycle-consistent adversarial networks”. *IEEE International Conference on Computer Vision (ICCV)*, 2242-2251, 2017.
- [5] Antipov G, Baccouche M, Dugelay J.-L. “Face aging with conditional generative adversarial networks”. *IEEE Conference on Image Processing (ICIP)*, 2089-2093, 2017.
- [6] Radford A, Metz L, Chintala S. “Unsupervised representation learning with deep convolutional generative Adversarial Networks”. *CoRR*, 1511, 06434, 2015.
- [7] Chen X, Duan Y, Houthoofd R, Schulman J, Sutskever I, Abbeel P. “Infogan: Interpretable representation learning by information maximizing generative adversarial nets”. *Advanced in Neural Information Processing Systems*, 2016.
- [8] Denton E, Chintala S, Szlam A, Fergus R. “Deep generative image models using a Laplacian pyramid of adversarial networks”, *Advanced in Neural Information Processing Systems*, 28, 2015.
- [9] Ledig C, Theis L, Huszár F, Caballero J, Cunningham A, Acosta A, Shi W. “Photo-realistic single image super-resolution using a generative adversarial network”, *IEEE Conference on Vision and Pattern Recognition (CVPR)*, 105-114, 2014.
- [10] Luo X, He X, Chen X, Qing L, Zhang J. “DualG-Gan, a dual-channel generator based generative adversarial network for text-to-face synthesis”, *Neural Networks*, 155, 155-167, 2022.
- [11] Kaggle. CelebFaces Attributes (CelebA) Dataset. <https://www.kaggle.com/datasets/jessicali9530/celeba-dataset> (01.09.2022).
- [12] Çelik G, Talu MF. “Çekişmeli üretken ağ modellerinin görüntü üretme performanslarının incelenmesi”. *Balıkesir Üniversitesi Fen Bilimleri Enstitüsü Dergisi*, 22, 181-192, 2020.
- [13] Shahriar S. “Gan Computers Generate Arts? A survey on visual arts, music, and literary text generation using generative Adversarial Network”. *Displays*, 73, 102237, 2022.



Investigation of flow properties and activation energy of magnesium lignosulfonate modified bitumen

Magnezyum lignosülfonat modifiyeli bitümün akış özelliklerinin ve aktivasyon enerjisinin araştırılması

Ahmet Münir ÖZDEMİR¹ , Bahadır YILMAZ^{2*} 

^{1,2}Civil Engineering, Engineering and Natural Sciences, Bursa Technical University, Bursa, Turkey.

¹ahmet.ozdemir@btu.edu.tr, ²bahadir.yilmaz@btu.edu.tr

Received: 10.11.2022
Accepted: 23.12.2022

Revision: 16.12.2022

doi: 10.5505/fujece.2023.79553
Research Article

Abstract

Recently, many studies have been carried out on the use of waste materials in bitumen modification. In this way, environmental and economic benefits are obtained and a field of use is created for waste materials. In this study, magnesium lignosulfonate (MLS), which is an organic waste material released during paper production from wood, was added to B50/70 bitumen. Penetration, softening point, rolling thin film oven test (RTFOT) and rotational viscometer (RV) tests were performed on modified binders. As a result of the experiments, it was determined that MLS increased the consistency, softening point and short-term aging resistance of the asphalt and decreased the temperature sensitivity. In addition, the activation energy values were determined using the Arrhenius equation and the flow properties were evaluated.

Keywords: Bitumen, Recycling, Organic additive, Lignin, Magnesium lignosulfonate

Özet

Son zamanlarda atık malzemelerin bitüm modifikasyonunda kullanımı konusunda çok sayıda çalışma yapılmıştır. Bu sayede çevresel ve ekonomik faydalar elde edilmekte, atık malzemeler için bir kullanım alanı oluşturulmaktadır. Bu çalışmada, odundan kağıt üretimi sırasında açığa çıkan ve organik bir atık madde olan magnezyum lignosülfonat B50/70 bitüme ilave edilmiştir. Magnezyum lignosülfonat (MLS) ilave edilmiş bağlayıcılar üzerinde penetrasyon, yumuşama noktası, dönel ince film halinde yaşlandırma (RTFOT) ve dönel viskozimetre (RV) deneyleri uygulanmıştır. Yapılan deneyler sonucunda MLS ilavesinin bitümün kıvamını, yumuşama noktasını ve kısa süreli yaşlanma direncini arttırdığı, sıcaklık hassasiyetini düşürdüğü tespit edilmiştir. Ayrıca Arrhenius denklemi kullanılarak aktivasyon enerjisi değerleri belirlenmiş, akış özellikleri değerlendirilmiştir.

Anahtar kelimeler: Bitüm, Geri dönüşüm, Organik katkı, Lignin, Magnezyum lignosülfonat

1. Introduction

Highways constitute the majority of the world's transportation network, and highways are generally built as flexible pavements. As it is known, flexible pavements generally consist of bituminous binder which obtained by refining petroleum and aggregate. Since these two materials are non-renewable, their overuse creates both economic and environmental consequences. Therefore, it is important to improve the properties of the materials used in the mixture and to reuse them with recycling approaches [1–6]. The most common method used to improve the properties of bituminous binders is the modification. With this method, various additives are added to the binder to improve its properties. The high quality bitumen obtained will make the pavement stronger against heavy and repetitive traffic loads, environmental effects, temperature differences [7–10]. A wide variety of additives can be used to modify the bitumen. The most commonly used additives are polymers such as Styrene butadiene styrene (SBS), Styrene isoprene SIS, Ethylene vinyl acetate (EVA) etc [11]. Studies have shown that these polymers, which are grouped as thermoplastic elastomer and plastomer, give very good results on bitumen performance [12–17]. However, the researchers focused on using waste materials in bitumen modification due to the difficulty of obtaining and expensive additive materials.

*Corresponding author

Industrial by-products emerge as a result of various productions, and these waste materials have negative effects on our environment. These materials, which cause a wide variety of pollution such as soil, water and air pollution, need to be used in various processes or recycled [18–20]. Recently, there have been many studies on the use of waste materials as a modifier for bitumen or hot mix asphalt (HMA) [4, 21–24]. In the study carried out by Shafabakhsh et al. for the use of waste rubber powders in HMA, the resistance to rutting was measured with a dynamic shear rheometer (DSR). In the results obtained, it was determined that the rubber powders added at the rate of 10% of the bitumen weight increase the resistance against rutting on the bitumen and increase the service life of the pavement [25]. Yan et al. inspected the rheological features of asphalt using waste tire rubber and ethylene vinyl acetate, one of the most widely used waste modifiers, and concluded that its high temperature performance was improved [26]. In addition, organic wastes are also used in bitumen modification and very successful results are obtained. Bostancıoğlu investigated the usability of activated carbon obtained from hazelnut shell wastes and furan resin obtained from vegetable wastes in bitumen modification. Both modified mixtures were noted to provide resistance to rutting and fatigue strength. It has also been stated that furan resin is a more resistant additive to moisture resistance compared to activated carbon [27, 28]. In another study, Yu et al. used waste packaging polyethylene (WPE) and organic montmorillonite (OMT) in asphalt modification and investigated the storage stability and rheological properties. WPE increased the rheological properties and permanent deformation resistance of the binder at high temperatures, while the combined use of WPE and OMT formed an exfoliated structure and increased the storage stability due to the high activity and adsorption properties of this structure [29].

Lignin is an organic molecule found in the structure of the cell wall together with cellulose and gives the plant its woody structure. Lignin, which is found in many trees and plants, enables the plant to stand upright and to transmit water to the higher leaves and branches by repelling water molecules. However, lignin is mostly encountered as a waste material in papermaking and is thrown into the environment as magnesium lignosulfonate as a result of the kraft method. Magnesium lignosulfonate (MLS) is an organic waste that is a dark liquid. However, lignin can provide various benefits when utilised in various applications. A major benefit is that it can absorb UV rays due to the benzene ring it contains. In addition, it can be used as a dispersion element for rubber materials due to its hydrophobic structure (benzene ring and carbon chain) [30–32].

In this study, magnesium lignosulfonate (MLS) obtained from lignin, which is a paper production waste, was used as a bitumen additive. In this context, it has been modified by adding 2, 4, 6 and 8% MLS to the bitumen. Then, conventional binder tests were applied and flow properties were determined by rotational viscometer test (RV). Flow characterization was supported by the activation energy value obtained by the Arrhenius equation.

2. Materials and Method

In the study, bitumen with a penetration grade of B50/70 supplied from Tüpraş İzmit Refinery and magnesium lignosulphate, a waste material from paper production, were used as additives. The physical properties of the bitumen used are given in Table 1.

Table 1. Properties of bitumen

Test	Standard	Value
Penetration (100g, 25°C, 5sn), dmm	ASTM D5	57
Softening point, °C	ASTM D36	50
Ductility (25°C, 5cm/min),cm	ASTM D113	100+
Flash point, °C	ASTM 92	248
Specific Gravity, (25°C), g/cm ³	ASTM D70	1,022
Fraass Breaking Point, °C	IP80	-10

Modified binders were obtained by adding 2%, 4%, 6% and 8% MLS to the pure binder, mixing at a mixing temperature of 155 °C and a speed of 1000 rpm. Penetration, softening point and rotational viscometer (RV) tests were carried out to determine the physical and rheological properties of modified asphalt binders. The viscosity values of the samples were obtained at 105°C, 135°C, 165°C, and 180°C using a Brookfield DV2T rotary viscometer device. RV test device was shown in Figure 1. Subsequently, to simulate short-term aging of pure and modified bitumens, Rolling Thin Film Oven Test (RTFOT) was performed. RV test was applied to RTFOT aged samples to determine flow characteristics of aged bitumens.



Figure 1. Rotational Viscometer (RV) test device

The resistance of the binder's molecules towards flow decreases with temperature increase, and molecules begin to move. In flowing liquids, the molecules that slide on each other must defeat the intermolecular forces that resist movement. This resistance power is called activation energy (E_a), and this value must be exceeded for the flow to begin [33, 34]. A large E_a value indicates that the viscosity of the bitumen is more sensitive to temperature [11]. This relationship is explained by the Arrhenius equation, and many successful studies have been carried out so far [35–37]. The Arrhenius equation was given in Equation 1.

$$\eta = A \times e^{\frac{E_a}{RT}} \quad (1)$$

Here, η is the viscosity of the binder (Pa.s), A is the regression coefficient, E_a is the activation energy (kJ/mol), T is the temperature of the test, and R is the universal constant of gas (8.314 J. mol⁻¹.K⁻¹).

3. Results

3.1. Penetration test results

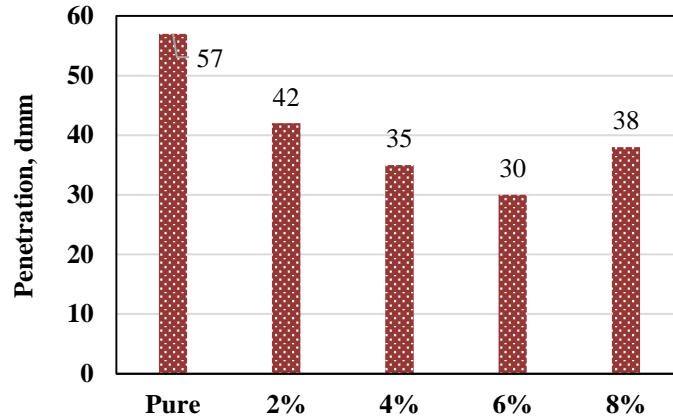


Figure 2. Penetration test results

Penetration test results of pure and 2, 4, 6 and 8% MLS modified bitumen was given in Figure 2. A regular decrease was observed in the penetration values up to the 6% additive addition, and the penetration value increased at the 8% additive addition. In general, it is seen that the penetration values of all samples increased compared to the pure binder. According to these results, it can be said that the additive hardens the bitumen. Using this bitumen will perform better at high temperatures and will provide higher strength than pure bitumen.

3.2. Softening point test results

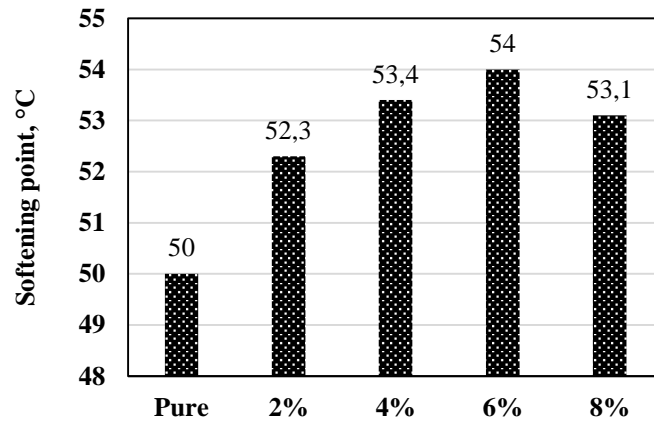


Figure 3. Softening point test results

The results of the softening point test applied to pure and modified binders are given in Figure 3. When Figure 3 is examined, a regular increase was observed until the addition of 6% additive, then this value decreased in the binder with 8% additive added. The results confirm the penetration test results. According to these results, it can be said that the additive material hardens the bitumen and starts to melt at higher temperatures.

3.3. Rotational Viscometer (RV) Test results

RV test results which performed on non-aged and RTFOT-aged samples was given in Figures 4 and 5. According to Figure 4 and Figure 5, the viscosity values of the binders decreased with the increase in temperature. As the temperature increased, the molecular mobility increased, the resistance to flow decreased. However, this decrease was limited by the increase in the contribution rate. In other words, the addition of MLS provided higher viscosity values than the pure binder at the same temperature. Viscosity values after RTFOT were higher than non-aged samples. With the volatilization of the light components in the bitumen, the heavy components increased proportionally, which increased the viscosity. At the same time, it is pleasing that the viscosity values are higher than the pure binder with the increase in the additive ratio. The higher the viscosity value, the higher the rutting resistance.

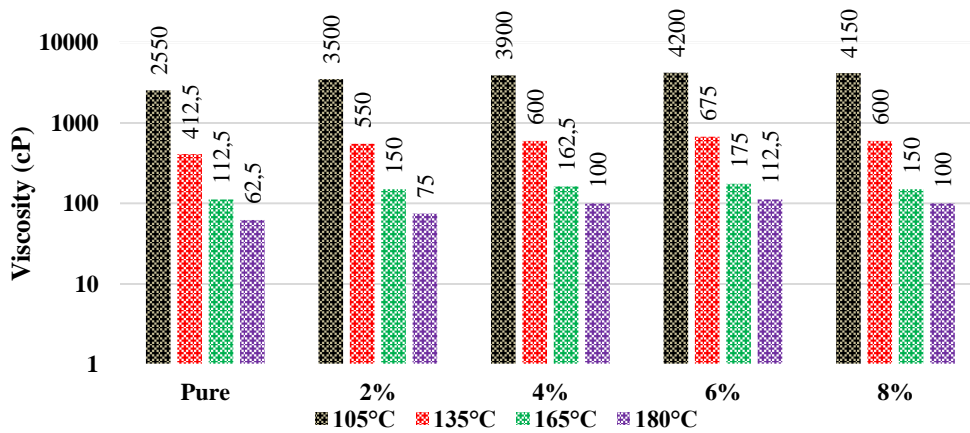


Figure 4. Rotational viscometer test results of non-aged pure and MLS modified binders

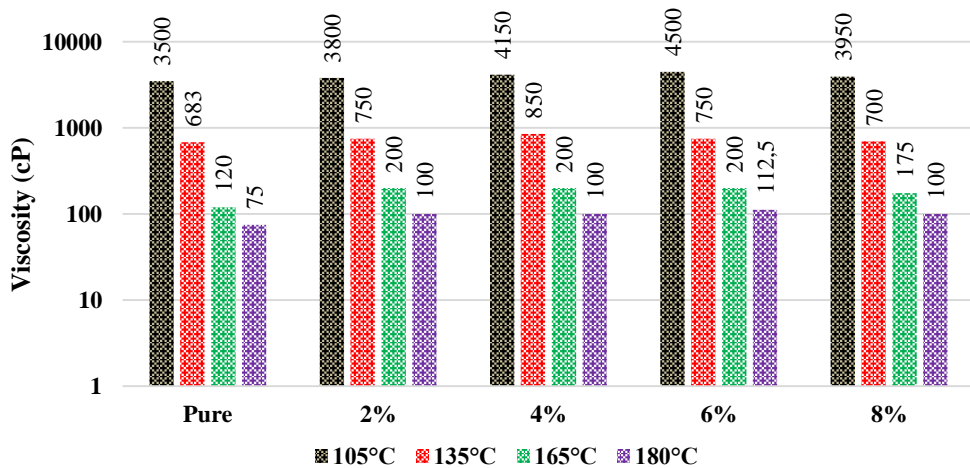


Figure 5. Rotational viscometer test results of RTFOT-aged pure and MLS modified binders

The activation energy (E_a) results which obtained by applying the Arrhenius equation to the viscosity values was given in Table 2. To see more clearly the effect of the additive ratio and the aging process Figure 6 was plotted.

Table 2. Activation energy values of non-aged and RTFOT aged bitumens

		Pure	2%	4%	6%	8%
Non-aged	E_a (kJ/mol)	68.681	68.224	67.738	67.699	69.399
	R^2	0.9414	0.9452	0.904	0.9272	0.8914
RTFOT-aged	E_a (kJ/mol)	76.203	72.24	71.21	70.451	70.388
	R^2	0.9609	0.9989	0.9894	0.9721	0.9829

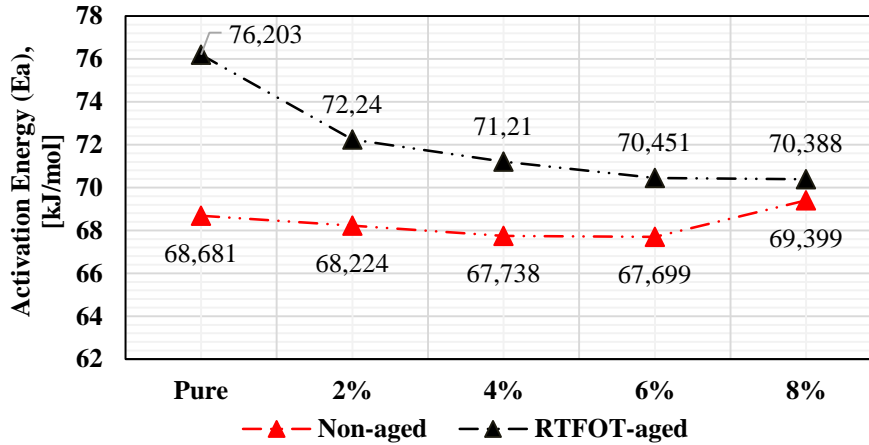


Figure 6. Activation energy (E_a) values of pure and modified binders

Activation energy is a threshold value that bitumen molecules must exceed in order to start moving [11]. Activation energy is an important parameter since the material needs to be liquefied for flexible pavement construction. An increase in this value means an increase in energy consumption. When Table 2 and Figure 6 are examined, the activation energy (E_a) value decreased with the increase in the additive ratio. It can be said that the decrease in E_a facilitated the occurrence of viscous flow. According to the traditional test results, it is seen that the material has hardened, but it has become easier for the material to take action for the flow phenomenon. Thanks to the activation energy analysis, in-depth evaluations can be made. It is seen that the E_a values after the RTFOT test increased compared to the unaged samples. The aging of the material adversely affected the flow character and increased the amount of energy required for flowing. However, it is pleasing that the E_a value decreases regularly with the use of additive. In general, it can be said that the material has become resistant to aging, in other words, it has not lost its flow properties despite aging.

4. Conclusion

In this study, the usability of magnesium lignosulfonate (MLS), a waste material released during paper production, in bitumen modification was investigated. For this purpose, 2%, 4%, 6% and 8% MLS were added to the pure bitumen and the effects were investigated. The results are given below in items:

- When the penetration test results were examined, it was observed that the penetration values of bitumen decreased with the increase in the additive ratio. This shows that the addition of MLS increases the consistency of the bitumen and increases its strength.
- According to the result of the softening point test, with the addition of MLS, the temperature value at which the bitumen starts to lose its properties, in other words, at which it starts to melt, has increased.
- RV results showed that the viscosity values of bitumen decreased with the increase in temperature values, but higher viscosity values were obtained compared to pure bitumen at the same temperature values with the use of MLS.

- According to the RV test performed on RTFOT-aged samples, the addition of MLS made the bitumen resistant to aging.
- Viscosity results are analyzed in depth with the Arrhenius equation. Activation energy values were obtained with the Arrhenius equation, and it was observed that the use of MLS caused a decrease in the activation energy values. A decrease in the activation energy means a decrease in the energy required for the bitumen to start flow.

In general, a usage area has been obtained for this waste material, which is released as a result of paper production. In this way, not only economic and environmental benefits are provided, but also the properties of the bituminous binder are improved.

5. Author Contribution Statement

Author 1 contributed to making the design, and the literature review contributed to forming the idea, and the analysis of the results. Author 2 contributed to conducting experimental studies, writing the article checking the spelling, and checking in terms of content.

6. Ethics Committee Approval and Conflict of Interest

There is no need for an ethics committee approval in the prepared article. There is no conflict of interest with any person/institution in the prepared article.

7. References

- [1] Hunter R, Self A, Read J. The Shell Bitumen Handbook, 6th edition. 2015.
- [2] Yalçın E. "Investigation of physical, chemical and rheological properties of bituminous binders modified with different rejuvenators". Journal of the Faculty of Engineering and Architecture of Gazi University, 37(1),497–510, 2021.
- [3] Vural Kök B, Aydoğmuş E, Yılmaz M, Akpolat M. "Investigation on the properties of new palm-oil-based polyurethane modified bitumen". Construction and Building Materials, 289,123152, 2021.
- [4] Kök BV, Yılmaz M, Akpolat M. "Performance evaluation of crumb rubber and paraffin modified stone mastic asphalt". Canadian Journal of Civil Engineering, 43(5),402–410, 2016.
- [5] Yılmaz M, Kök BV, Kulolu N. "Effects of using asphaltite as filler on mechanical properties of hot mix asphalt". Construction and Building Materials, 25(11),4279–4286, 2011.
- [6] Oruç Ş, Yılmaz B. "Improvement in performance properties of asphalt using a novel boron-containing additive". Construction and Building Materials, 123,207–213, 2016.
- [7] Fini EH, Hajikarimi P, Rahi M, Moghadas Nejad F. "Physiochemical, Rheological, and Oxidative Aging Characteristics of Asphalt Binder in the Presence of Mesoporous Silica Nanoparticles". Journal of Materials in Civil Engineering, 28(2),04015133, 2016.
- [8] Rahbar-Rastegar R, Daniel JS, Dave E V. "Evaluation of Viscoelastic and Fracture Properties of Asphalt Mixtures with Long-Term Laboratory Conditioning". Transportation Research Record: Journal of the Transportation Research Board, 2672(28),503–513, 2018.
- [9] Zaniwski J, Pumphrey M. "Evaluation of Performance Graded Asphalt Binder Equipment and Testing Protocol". 2004.
- [10] Notani MA, Arabzadeh A, Satvati S, Tarighati Tabesh M, Ghafari Hashjin N, Estakhri S, *et al.* "Investigating the high-temperature performance and activation energy of carbon black-modified asphalt binder". SN Applied Sciences, 2(2),303, 2020.
- [11] Yılmaz B, Özdemir AM, Gürbüz HE. "Assessment of Thermal Properties of Nanoclay-Modified Bitumen". Arabian Journal for Science and Engineering, 2022.
- [12] Zhang F, Hu C. "The research for SBS and SBR compound modified asphalts with polyphosphoric acid and sulfur". Construction and Building Materials, 43,461–468, 2013.
- [13] Ameri M, Mohammadi R, Mousavinezhad M, Ameri A, Shaker H, Fasihpour A. "Evaluating Properties of Asphalt Mixtures Containing polymers of Styrene Butadiene Rubber (SBR) and recycled Polyethylene Terephthalate (rPET) against Failures Caused by Rutting, Moisture and Fatigue". Frattura ed Integrità Strutturale, 14(53),177–186, 2020.
- [14] Mahmoud Ameri, Reza Mohammadi, Milad Mousavinezhad, Amirhossein Ameri, Hamid Shaker, Arash Fasihpour. "Evaluating Properties of Asphalt Mixtures Containing polymers of Styrene Butadiene Rubber (SBR) and recycled Polyethylene Terephthalate (rPET) against Failures Caused by Rutting, Moisture and Fatigue". Frattura ed Integrità Strutturale, 14(53),177–186, 2020.
- [15] Ameri M, Mansourian A, Sheikhmotevali AH. "Laboratory evaluation of ethylene vinyl acetate modified bitumens and

- mixtures based upon performance related parameters". *Construction and Building Materials*, 40,438–447, 2013.
- [16] Chegenizadeh A, Tokoni L, Nikraz H, Dadras E. "Effect of ethylene-vinyl acetate (EVA) on stone mastic asphalt (SMA) behaviour". *Construction and Building Materials*, 272,121628, 2021.
- [17] Siddig EAA, Feng CP, Ming LY. "Effects of ethylene vinyl acetate and nanoclay additions on high-temperature performance of asphalt binders". *Construction and Building Materials*, 169,276–282, 2018.
- [18] Ameli A, Maher J, Mosavi A, Nabipour N, Babagoli R, Norouzi N. "Performance evaluation of binders and Stone Matrix Asphalt (SMA) mixtures modified by Ground Tire Rubber (GTR), waste Polyethylene Terephthalate (PET) and Anti Stripping Agents (ASAs)". *Construction and Building Materials*, 251,118932, 2020.
- [19] Xue Y, Hou H, Zhu S, Zha J. "Utilization of municipal solid waste incineration ash in stone mastic asphalt mixture: Pavement performance and environmental impact". *Construction and Building Materials*, 23(2),989–996, 2009.
- [20] Alsheyab MAT, Khedaywi TS. "Effect of electric arc furnace dust (EAFD) on properties of asphalt cement mixture". *Resources, Conservation and Recycling*, 70,38–43, 2013.
- [21] Behnood A, Modiri Gharehveran M. "Morphology, rheology, and physical properties of polymer-modified asphalt binders". *European Polymer Journal*, 112,766–791, 2019.
- [22] Sengoz B, Topal A. "Use of asphalt roofing shingle waste in HMA". *Construction and Building Materials*, 19(5),337–346, 2005.
- [23] Li J, Chen Z, Xiao F, Amirkhani SN. "Surface activation of scrap tire crumb rubber to improve compatibility of rubberized asphalt". *Resources, Conservation and Recycling*, 169,105518, 2021.
- [24] Ma J, Hu M, Sun D, Lu T, Sun G, Ling S, *et al.* "Understanding the role of waste cooking oil residue during the preparation of rubber asphalt". *Resources, Conservation and Recycling*, 167,105235, 2021.
- [25] Shafabakhsh GH, Sadeghnejad M, Sajed Y. "Case study of rutting performance of HMA modified with waste rubber powder". *Case Studies in Construction Materials*, 1,69–76, 2014.
- [26] Yan K, Chen J, You L, Tian S. "Characteristics of compound asphalt modified by waste tire rubber (WTR) and ethylene vinyl acetate (EVA): Conventional, rheological, and microstructural properties". *Journal of Cleaner Production*, 258,120732, 2020.
- [27] Bostancıoğlu M, Oruç Ş. "Effect of activated carbon and furan resin on asphalt mixture performance". *Road Materials and Pavement Design*, 17(2),512–525, 2016.
- [28] Bostancıoğlu M, Oruç Ş. "Effect of furfural-derived thermoset furan resin on the high-temperature performance of bitumen". *Road Materials and Pavement Design*, 16(1),227–237, 2015.
- [29] Yu R, Fang C, Liu P, Liu X, Li Y. "Storage stability and rheological properties of asphalt modified with waste packaging polyethylene and organic montmorillonite". *Applied Clay Science*, 104,1–7, 2015.
- [30] Pérez IP, Rodríguez Pasandín AM, Pais JC, Alves Pereira PA. "Use of lignin biopolymer from industrial waste as bitumen extender for asphalt mixtures". *Journal of Cleaner Production*, 220,87–98, 2019.
- [31] Liu X, Wang J, Li S, Zhuang X, Xu Y, Wang C, *et al.* "Preparation and properties of UV-absorbent lignin graft copolymer films from lignocellulosic butanol residue". *Industrial Crops and Products*, 52,633–641, 2014.
- [32] Xiao S, Feng J, Zhu J, Wang X, Yi C, Su S. "Preparation and characterization of lignin-layered double hydroxide/styrene-butadiene rubber composites". *Journal of Applied Polymer Science*, 130(2),1308–1312, 2013.
- [33] Salomon D, Zhai H. "Asphalt binder flow activation energy and its significance for compaction effort". *Proceedings of the 3rd Eurasphalt and Eurobitume congress held Vienna, May 2004*, (1),1754–1762, 2004.
- [34] Abed YH, Abedali Al-Haddad AH. "Temperature Susceptibility of Modified Asphalt Binders". *IOP Conference Series: Materials Science and Engineering*, 671(1) 2020.
- [35] Zhang L, Liu Q, Wu S, Rao Y, Sun Y, Xie J, *et al.* "Investigation of the flow and self-healing properties of UV aged asphalt binders". *Construction and Building Materials*, 174,401–409, 2018.
- [36] Jin D, Wang J, You L, Ge D, Liu C, Liu H, *et al.* "Waste cathode-ray-tube glass powder modified asphalt materials: Preparation and characterization". *Journal of Cleaner Production*, 314,127949, 2021.
- [37] Jiang X, Li P, Ding Z, Yang L, Zhao J. "Investigations on viscosity and flow behavior of polyphosphoric acid (PPA) modified asphalt at high temperatures". *Construction and Building Materials*, 228,116610, 2019.